From
the Department of Clinical Science, Intervention and Technology
the Division of Medical Imaging and Technology
Karolinska Institutet, Stockholm, Sweden

DRUG AND DISEASE EFFECTS ON THE HUMAN BRAIN STUDIED BY FUNCTIONAL MRI

Love Engström Nordin

Karolinska Institutet

Stockholm 2016

All previously published papers were reproduced with permission from the publisher.
Cover image created by Ebba Nordin 2016, reproduced with permission from the artist.
Published by Karolinska Institutet.
Printed by E-PRINT AB 2016

ISBN 978-91-7676-314-8

Drug and disease effects on the human brain studied by functional MRI

THESIS FOR DOCTORAL DEGREE (Ph.D.)

By

Love Engström Nordin

Principal Supervisor:
Professor Tie-Qiang Li
Karolinska Institutet
Department of Clinical Science, Intervention and Technology
Division of Medical Imaging and Technology

Co-supervisor:
Doctor Per Julin
Karolinska Institutet
Department of Clinical Sciences, Danderyd Hospital
Division of Rehabilitation Medicine

Opponent:
PhD Atsushi Takahashi
Massachusetts Institute of Technology, Boston
Department of McGovern Institute
Division of Martinos Imaging Center, MIT

Examination Board:
Associate professor Gunther Helms
Lund University
Department of Clinical Sciences
Division of Medical Radiation Physics, Lund

Associate professor Peter Leander
Lund University
Department of Translational Medicine
Division of Radiology Diagnostics, Malmö

Professor Svein Kleiven
Royal Institute of Technology, Stockholm
Department of School of Technology and Health
Division of Neuronic Engineering

To Linnea and Ebba

ABSTRACT

Background: With the advent of magnetic resonance imaging (MRI) technology, various functional MRI (fMRI) techniques have become available for non-invasive neuroscientific studies and clinical diagnostics, which have led to a better understanding of the human brain function in normal and diseased subjects. In order to interpret the fMRI results correctly and design optimal research studies it is important to understand both the potentials and limitations associated with each fMRI technique. In this thesis we used two fMRI techniques: arterial spin labeling (ASL) and resting-sate BOLD (blood-oxygen-level dependent) fMRI to study the effects of a CNS-active (central nervous system) drug and neurologic disorder on the human brain function.

Purpose: The main research purposes of this thesis are the following: 1) We assess the reproducibility and reliability of rCBF (regional cerebral blood flow) measurements conducted at 3T with pCASL (pseudo continuous ASL) technique; 2) We study the pharmacokinetics of a CNS active drug in normal volunteers by conducting rCBF measurements as a function of time after intake of a single dose of 20 mg d-amphetamine with the pCASL technique; 3) We investigate the possible neurological abnormalities of mild traumatic brain injury (mTBI) patients with chronic fatigue by performing rCBF and resting-sate functional connectivity measurements before, during and after a 20 minute continuous psychomotor vigilance task (PVT).

Conclusion: The results from these studies show that the pCASL technique is a relatively robust method for quantitative measurements of rCBF in both normal volunteers and patient subjects. Repeated rCBF measurements with the pCASL method is a non-invasive and sufficiently sensitive approach to assess pharmacokinetic response to CNS active chemicals and should be useful for studying the neurophysiological characteristics *in vivo* of potential CNS drugs. The results from the mTBI subjects demonstrate that the repeated measurements of rCBF and functional connectivity metrics before, during and after a PVT provide sensitive diagnostic imaging methods to assess neurological abnormality of mTBI patients without apparent neuroanatomical damage. In addition to the clinical diagnostic value, these studies also contribute to important knowledge for the design and analysis of brain functional imaging studies of drugs and neurological diseases.

SAMMANFATTNING

Bakgrund: Den snabba utvecklingen av bildgivande MR (magnetresonans) har resulterat i att flera olika funktionella MR-metoder blivit tillgängliga för bland annat icke-invasiva neurovetenskapliga studier och klinisk diagnostik. Metoderna har bidragit till bättre förståelse av den mänskliga hjärnan i sjukt och friskt tillstånd. För att kunna tolka funktionella MR-resultat på ett korrekt sätt och för att kunna utforma produktiva forskningsstudier är det viktigt att ha god insikt i både de möjligheter och begränsningar som förekommer med funktionella MR-tekniker. I den här avhandlingen har vi använt två olika funktionella MR-tekniker: ASL (eng. arterial spin labeling) och resting-state BOLD (eng. blood-oxygen-level dependent) funktionell MR för att studera effekten av CNS-aktiva (centrala nervsystemet) läkemedel och neurologiska tillstånd på den mänskliga hjärnans funktion.

Syfte: De huvudsakliga syftena med den här avhandlingen är: 1) Att utvärdera reproducerbarheten och tillförlitligheten för regionala cerebrala blodflödesmätningar (rCBF) utförda i ett 3T MR-system med pCASL-tekniken (eng. pseudo continuous ASL); 2) Att studera de farmakokinetiska egenskaperna för ett CNS-aktivt läkemedel hos friska försökspersoner genom att utföra rCBF-mätningar som funktion av tid efter intag av 20 mg d-amfetamin med pCASL-metoden; 3) Att utvärdera möjliga neurologiska avvikelser hos patienter med lätta traumatiska hjärnskador som lider av kronisk trötthet genom att mäta rCBF och funktionell konnektivitet under vila med funktionell MR före, under och efter ett 20 minuter långt psykomotoriskt vigilanstest.

Slutsats: Resultaten från dessa studier visar att pCASL är en relativt robust teknik för kvantitativa mätningar av rCBF hos både friska försökspersoner och patienter. Upprepade mätningar av rCBF med pCASL är en icke-invasiv metod som är tillräckligt känslig för att mäta den farmakokinetiska responsen från CNS-aktiva läkemedel och för att studera det neurofysiologiska förloppet *in vivo* för potentiella CNS-läkemedel. Resultaten från patienterna med lätta traumatiska hjärnskador visar att upprepade mätningar av rCBF och funktionell konnektivitet före, under och efter ett psykomotoriskt vigilanstest utgör känsliga diagnostiska bildgivande metoder för att utvärdera neurologiska avvikelser hos patienter utan uppenbara neuroanatomiska skador. Utöver den kliniska nyttan, bidrar dessa studier till viktig kunskap för att kunna utforma och analysera bildgivande forskningsstudier inom läkemedel och neurologiska sjukdomstillstånd.

LIST OF SCIENTIFIC PAPERS

I. **Inter- and intra-subject variability of brain perfusion measurements using pseudo continuous arterial spin labeling (pCASL) technique at 3T** Tie-Qiang Li, Love Engström Nordin
Manuscript

II. **Cortical responses to amphetamine exposure studied by pCASL and pharmacokinetic/pharmacodynamic dose modeling** Love Engström Nordin, Tie-Qiang Li, Jakob Brogren, Patrik Johansson, Niclas Sjögren, Kristin Hannesdottir, Charlotta Björk, Märta Segerdahl, Danny J.J. Wang, Per Julin
NeuroImage 2013;68:75-82. doi:10.1016/j.neuroimage.2012.11.035

III. **Post mTBI fatigue is associated with abnormal brain functional connectivity** Love Engström Nordin, Marika C. Möller, Per Julin, Aniko Bartfai, Farouk Hashim, Tie-Qiang Li
Scientific Reports 6, Article number: 21183 (2016). doi:10.1038/srep21183

IV. **Neural activity during vigilance test performance– relation to cognitive fatigability in mild TBI** Marika C. Möller, Love Engström Nordin, Tie-Qiang Li, Aniko Bartfai, Per Julin
Manuscript

CONTENTS

LIST OF ABBREVIATIONS

1D / 2D / 3D	One- / two- / three-dimensional
ANOVA	Analysis of variance
P- / C- / pC- ASL	Pulsed-/continuous-/pseudo continuous- arterial spin labeling
α	Labeling efficiency
B_0 / B_1	Static magnetic field / oscillating magnetic field
$B_1^e(t)$	Pulse envelope function
BOLD	Blood-oxygen-level dependent
bw	Band width
(r)CBF	(regional) Cerebral blood flow
CNS	Central nervous system
CSF	Cerebrospinal fluid
CV	Coefficient of variation
$E_\uparrow$ / $E_\downarrow$	Parallel spin (up) / antiparallel spin (down)
EPI	Echo planar imaging
E_{rf}	Energy of RF-field
G	Gradient
GLM	General linear model
GM / WM	Gray matter / white matter
γ	Gyromagnetic constant
$\hbar$	Dirac's constant
I	Spin state
j	Total angular momentum
K	Boltzmans constant
k-space	Raw-data matrix
k_x / k_y	x- / y-direction in k-space
l	Orbital angular momentum
λ	Blood/tissue water partition coefficient
M_0	Signal from blood at equilibrium
$\vec{M}$	Magnetization vector

$\vec{M}_z$	Magnetization vector along the z-direction
$\vec{M}_{xy}$	Magnetization vector in xy-plane
ΔM	Signal difference from pair-wise image subtraction
(f)MRI	(functional) Magnetic resonance imaging
MT	Magnetic transfer
mTBI	Mild traumatic brain injury
$\vec{\mu}$	Magnetic moment
N_s	Total number of spins
NMR	Nuclear magnetic resonance
υ_{max}	Highest occurring frequency
ω	Post labeling delay time
ω_0	Larmor frequency
ω_{rf}	Frequency of RF-pulse
PET	Positron emission tomography
PVT	Psychomotor vigilance task
φ	Phase
QA	Quality assurance
R_{1a}	Longitudinal relaxation rate of blood
RF	Radio frequency
s	Spin
SNR	Signal to noise ratio
T_1 / T_2	Longitudinal- / transversal- relaxation time constant
T_2*	Effective T_2 reflecting spin-spin interactions and B_0-inhomogeneities
T_s	Temperature in a spin system
τ	Labeling time
VAS-f	Visual analog scale of fatigue
x-, y-, z-direction	Coordinate system (spin system / location in MRI scanner)
xy-plane	Transverse plane: area between the x- and y-axis in a spin system
Δx	Slice width

1 INTRODUCTION

1.1 A BRIEF HISTORY OF MRI IN MEDICINE

The road to magnetic resonance imaging (MRI) has resulted in several Nobel prizes. The first was handed out in physics 1952 to Felix Bloch and Edward M. Purcell with the following motivation: "for their development of new methods for nuclear magnetic precision measurements and discoveries in connection therewith". This was followed by 2 Nobel prizes in chemistry (Richard R. Ernst 1991 and Kurt Wüthrich 2002) for the development of NMR techniques. The Nobel Prize in medicine for the discoveries concerning magnetic resonance imaging was awarded to Paul C. Lauterbur and Sir Peter Mansfield in 2003. The first clinically usable image from a whole body MRI scanner was produced in 1980 at the University of Aberdeen, UK, since then the use of MRI in medicine has increased almost exponentially worldwide. Today MRI is routinely used for clinical diagnoses at most hospitals and the technique is also very important for medical research in a large variety of medical research areas. MRI is a powerful technique offering excellent soft-tissue contrast. It can be used for morphological and functional imaging, checkups and quantitative measurements. Unlike x-ray and nuclear medicine methods, MRI does not expose the patients to any kind of ionizing radiation.

1.2 BASIC PHYSICS OF MRI

In MRI the resonance phenomenon of nuclear spins is exploited to detect a signal that can be used to reconstruct medical images. In order to generate this signal the subject of interest needs to be exposed to an external magnetic field. The basic physics behind MRI will be briefly described in the following sections.

1.2.1 Nuclear spin

Each atomic nucleus consists of nucleons, more particularly protons and neutrons. Nucleons have an intrinsic spin, described as the angular momentum of the nucleon. The total angular momentum of a nucleon, *j*, can be described by the following equation:

$$j = l + s \tag{1}$$

where *l* is the orbital angular momentum and *s* is the spin. The total angular momentum of a nucleus i.e. the nuclear spin (*I*) is obtained by the vector sum of the angular momenta of all nucleons. The value that *I* assume for a particular nucleus in its ground state follows the rules stated in table 1.

Table 1 Nuclear spin, *I*, as a function of mass- and charge number.

Mass number, A	Charge number, Z	Nuclear spin, *I*
Even	Even	0
Odd	Even	Half-integer
Even	Odd	Integer
Odd	Odd	Half-integer

All atomic nuclei have electrical charges. A rotating charged particle will give rise to a magnetic field. The spin and magnetic moment ($\vec{\mu}$) vectors are related to each other by:

$$\vec{\mu} = \gamma I \tag{2}$$

where γ is a physical constant called gyromagnetic ratio. In the absence of an external magnetic field (B_0) the direction of $\vec{\mu}$ is random at room temperature because of thermal motion.

In the presence of a B_0-field the nuclear Zeeman effect can be observed where the nuclear spin state, I, is split up into $2I+1$ individual sub states. In MRI the most frequently used nucleus is hydrogen, consisting of a single proton. The hydrogen nucleus has a nuclear spin of ½ which means that in the presence of a static magnetic field, the nucleus spin splits up into 2 possible sub states. The orientation of the magnetic moment vector for the two described sub states are often denoted as spin up (parallel, $E_\uparrow$) or spin down (antiparallel, $E_\downarrow$). The energy difference between these sub states is given by:

$$\Delta E = E_\downarrow - E_\uparrow = \gamma \hbar B_0 \tag{3}$$

where $\hbar$ is Dirac's constant. Spin up is the lower energy state and spin down is the higher energy state.

From the quantum mechanical point of view a hydrogen nucleus can take any linear combination between the two sub states, however, in the scope of this thesis, classical physics will be sufficient to describe the basic physics of MRI. According to classical physics, in the presence of an external magnetic field the magnetic moment vector, $\vec{\mu}$, of a nuclear spin will experience a torque from the B_0 field. The torque that $\vec{\mu}$ experiences gives rise to nuclear precession (figure 1). The angular frequency of this nuclear precession, often called the Larmor frequency (ω_0), can be calculated by:

$$\omega_0 = \gamma B_0 \tag{4}$$

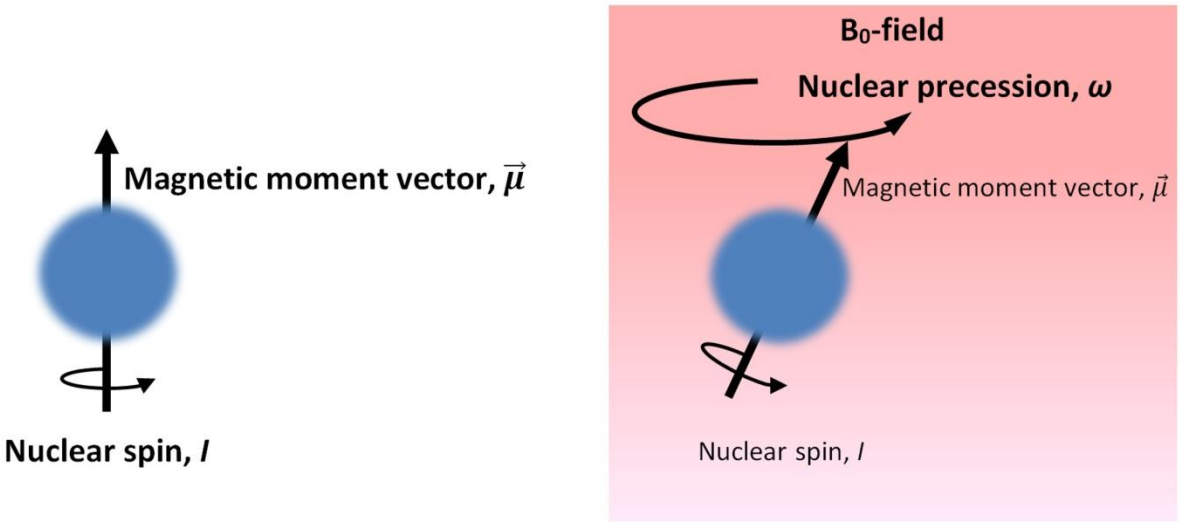

Figure 1 In the presence of an external magnetic field, nuclear precession takes place for any nucleus with a non-zero spin.

1.2.2 Nuclear Magnetic Resonance (NMR)

When a macroscopic sample is exposed to an external magnetic field at room temperature it is slightly more likely for a nucleus spin to be in the lower energy state (parallel) than the higher energy state (anti-parallel) as can be predicted by the Boltzmann distribution. The vector sum of all magnetic moments in a sample is called the magnetization vector, $\vec{M}$. At thermal equilibrium, $\vec{M}$ aligns along the positive B_0-direction, typically denoted as z-direction, and is given by:

$$\vec{M} = M_x\vec{\imath} + M_y\vec{\jmath} + M_z\vec{k} \tag{5}$$

where $M_x\vec{\imath}$ and $M_y\vec{\jmath}$ is zero. In the xy-plane, or transverse plane, the projection of $\vec{\mu}$ has a random phase resulting in zero magnetization. The magnitude of $\vec{M}$ can be calculated by:

$$M_z^0 = \left|\vec{M}\right| = \frac{\gamma^2\hbar^2 B_0 N_s}{4KT_s} \qquad \text{(spin-½ system)} \tag{6}$$

where N_s is the total number of spins, T_s is the temperature in the spin system and K is Boltzmanns constant. It is clear that the magnitude of $\vec{M}_z^0$ is directly proportional to B_0. In order to obtain magnetization in the transverse plane, phase coherence must be established. This can be achieved by applying an oscillating magnetic field (B_1 / RF-field), usually referred to as a RF-pulse. This B_1-field, generated perpendicularly to the B_0-field, can be described by:

$$B_1(t) = B_1^e(t)e^{-i(\omega_{rf}t+\varphi)} \tag{7}$$

where $B_1^e(t)$ is the pulse envelope function which specifies the shape and duration of the RF-pulse and φ is the initial phase. The energy of the RF-field, E_{rf}, is given by:

$$E_{rf} = \hbar\omega_{rf} \tag{8}$$

where ω_{rf} is called the excitation carrier frequency i.e. the frequency of the RF-pulse. The energy of the RF-field must be equal to the energy difference between the spin up and spin down states:

$$\hbar\omega_{rf} = \Delta E = \gamma\hbar B_0 \rightarrow \omega_{rf} = \omega_0 \tag{9}$$

In the view of classical physics, when the RF-field has the same frequency as the precession of the spins, a measurable net magnetization ($\vec{M}_{xy}$) can be established in the transverse plane. The angle between $\vec{M}_{xy}$ and the z-axis is called the flip angle. The flip angle depends on the magnitude and duration of the B_1-field and is therefore defined by the pulse envelope function.

1.2.3 The NMR relaxation phenomenon

Following a RF-excitation pulse the spins will eventually return to their thermal equilibrium state and the net magnetization realign with the B_0-direction. This process is called NMR relaxation and has two basic components; longitudinal- and transversal relaxation. The longitudinal relaxation (T1-relaxation) describes the return of $\vec{M}$ to the lower energy state, along B_0. During T1 relaxation nucleons dissipate energy as heat to the surrounding matter. The transversal relaxation (T2-relaxation) describes the decay of the phase coherence among the precessing nucleons in the xy-plane. This decay occurs because of spin-spin interactions between the nucleons (T2) and because of macroscopic inhomogeneity's in the B_0-field (T2*). Both the longitudinal and transversal relaxations typically follow an exponential function and can be described by the following equations:

$$M_z(t) = M_z^0(1 - e^{-t/T1}) \quad \text{(longitudinal)} \tag{10}$$

$$M_{xy}(t) = M_{xy}e^{-t/T2} \quad \text{(transversal)} \tag{11}$$

Where T_1 is the decay time constant for the recovery of the *z* component of the nuclear spin magnetization and T_2 is the decay time constant for the component in the transverse plane. The time constant T1 is approximately the time that takes for 63% of the *z* component to recover after a 180º inversion. Likewise T2 can be approximately considered as the time after which only 37% of M_{xy} remains after an initial 90º excitation. The T1- and T2 relaxation times differ typically in biological tissues, resulting from the differences in chemical composition, microscopic structure, and physiological status. This provides a very powerful

approach to use the T1 and T2 relaxation contrasts to differentiate between different types of tissues. Because of the excellent soft tissue contrast, T1- and T2-weighted MRI are routinely used for diagnostics of soft tissue pathology.

1.2.4 Signal detection and the MRI system

We now know that a net magnetization vector, $\vec{M}_z$, exists when a spin system is exposed to a static magnetic field, B_0. The spins composing $\vec{M}_z$ can be excited with an alternating radio frequency (RF) electromagnetic field resulting in a transverse magnetization component, $\vec{M}_{xy}$. The transverse magnetization vector will decrease with time following the T1- and T2 relaxation mechanisms, until M_z is fully recovered as in the thermal equilibrium condition. This process can be monitored and partly manipulated in order to acquire sufficient information to produce images for medical diagnosis. According to Faraday´s law of induction that states an oscillating electromagnetic field will induce a current in an electric circuit, the coherent precession of all spins composing $\vec{M}_{xy}$ after excitation of the spin system generates an oscillating electromagnetic field that can, therefore, be measured by a volt-meter connected to an induction coil.

As described by equation 4, the precession frequency is dependent on the strength of the static magnetic field, B_0. The applied RF-pulse, B_1, needs to have the same frequency as the precession of the nuclear spins to establish a resonance condition (equation 9). Taking advantage of this resonance phenomenon of the nuclear spin system, the gradient system in a MRI scanner can generate variations of the magnetic field strength in the x-, y, or z-direction, or their linear combinations. By applying a gradient during excitation with a RF-pulse corresponding to a specific limited frequency range (bandwidth, bw) it is possible to excite only a thin slice of an object at a given position within the gradient field in the MRI scanner. The relation between bw, slice thickness (Δx) and gradient strength (G) is given by:

$$bw = \frac{\gamma}{2\pi} \cdot G \cdot \Delta x \tag{12}$$

The gradient used to define a slice is often called slice selection gradient. The gradient system is also used for imaging by two different methods called the frequency- and phase encodings. The frequency encoding gradient is turned on during signal readout and, therefore, the induced spatial frequency shift in the excited slice is registered. After the slice selection the magnetization vector is transformed in the xy-plane, before the signal read out, a phase encoding gradient is applied for a short time period. The phase encoding gradient introduces a spatially varying phase angle for the spins different locations along the phase encoding gradient. Using the slice selection-, frequency-, and phase encoding techniques described above, sufficient information can be acquired to construct 2D images. To acquire a slab of slices the slice selection gradient and RF excitation pulse are changed between each slice. In 3D imaging the amplitude of slice selection gradient and RF bandwidth are adjusted according eq. 12 to cover the entire imaging volume. Furthermore, a second phase encoding

gradient has to be implemented to resolve the spatial information along the third direction. The scheme to implement a combination of magnetic field gradient pulses and RF-pulses to generate enough signal to produce a magnetic resonance image is called a MRI pulse sequence. By controlling the exact timing of the pulse sequence images of different contrast can be created from the acquired signal. The recorded analog signal is typically amplified, and digitized, demodulated, and filtered before image reconstruction. The high-frequency signal (~100 MHz) is converted in the demodulator (a part of the receiver) to a low frequency (100 kHz to 1 MHz) signal that contains the information with the frequency range across the field of view encoded by the frequency encoding gradient. The demodulated signal is sampled as a function of time with a minimum sampling frequency criterion determined by:

$$1/T = 2 \cdot \upsilon_{max} \qquad \text{(Nyquist frequency)} \tag{13}$$

where T is the sampling dwell time and the corresponding Nyquist frequency, υ_{max}, should be higher than the highest occurring frequency in the demodulated signal. Any slower sampling rate would result in aliasing artifacts. The image raw-data can be conveniently represented in a mathematical form called k-space, where each data point in the time-domain contains the amplitude and frequency information of the acquired signal. For conventional 2D MRI each row in k-space (k_x) corresponds to a frequency readout following a phase encoding step. The entire k-space plane is adequately sampled line-by-line while stepping the phase encoding gradient systematically from the system minimum to maximum. This rectilinear line-by-line signal sampling trajectory is called Cartesian sampling. Other non-rectilinear trajectories, such as, spiral and rotating blade, are also used in more advanced MRI. Each data point in k-space contains information about the signal amplitude and frequency necessary to reconstruct the final real space image with meaningful contrast information. It can be demonstrated that the k-space data and real-space images are mathematically related by a Fourier transformation. Therefore, by performing an inverse Fourier transform on the k-space raw data, the real space medical image can be constructed, where the intensity of each pixel is related to the amplitude of the sampled time-domain signal (figure 2).

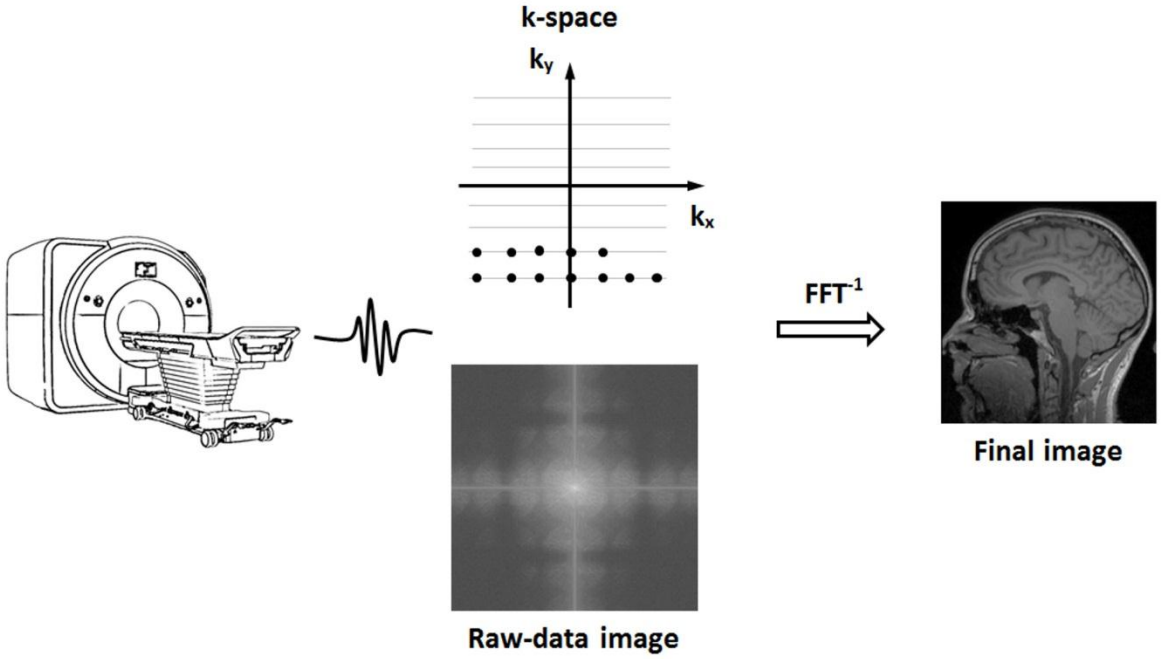

Figure 2 Schematic overview of MRI. The acquired signal is used to fill k-space with phase- and frequency information which is constructed to the final image through inverse Fourier transformation.

1.3 FUNCTIONAL MRI TECHNIQUES

The human brain is constantly active at a neural level regardless of whether you are performing a cognitive or physical task or are at rest. Neural activity is reflected in the hemodynamic response regulating the blood flow in the brain (Buxton, Uludağ, Dubowitz, & Liu, 2004). Functional MRI studies often use the blood-oxygen-level dependent (BOLD) fMRI experimental techniques where the brain activity is monitored during the performance of certain tasks inside the MRI scanner. The concept of fMRI though is more comprehensive since the emergence and improvement of several new techniques and their applications in neuroscience studies. In this thesis the focus will be on the application of the arterial spin labeling (ASL) technique and resting-state BOLD fMRI. ASL provides the possibility of quantitative measurements of the cerebral perfusion making it possible to monitor the direct hemodynamic response following brain activity. Resting-state BOLD fMRI is a technique suitable for studying the characteristics of temporal fluctuations between different brain regions during resting-state, which is an area of research that has attracted increased attention in recent years, because of its potential applicability both in healthy and diseased populations.

1.3.1 ASL

Arterial spin labeling is a non-invasive quantitative technique for measuring blood perfusion (Williams, Detre, Leigh, & Koretsky, 1992). Perfusion in the brain tissue measured by ASL can be specified in terms of ml of blood per 100 gram of tissue per unit of time (ml/100g/min). The basic procedure of the ASL method include 1) labeling of the magnetization of the arterial blood flowing into the brain, 2) a time delay allowing the labeled blood to flow into the capillaries of the brain tissues, 3) a fast (single-shot) image acquisition of the brain, 4) acquisition of an unlabeled control image, 5) subtraction of the labeled and

control images for the quantification of blood perfusion. There are two basic types of ASL techniques, continuous ASL (CASL) and pulsed ASL (PASL) (Golay, Hendrikse, & Lim, 2004).

In CASL a spatially localized continuous RF-field inverts the incoming spins of the arterial blood in the presence of a slice selection gradient, typically for a few seconds (Detre et al., 1994; Williams et al., 1992; Zhang, Williams, & Koretsky, 1993). The inversion RF-field is applied to a labeling plane perpendicularly to the major arteries entering the brain. A separate local surface coil is usually used for this labeling purpose (Silva, Zhang, Williams, & Koretsky, 1995; Zhang, Silva, Williams, & Koretsky, 1995). When the labeled proton spins in the arterial blood enters the brain it still has a certain degree of inverted longitudinal magnetization causing a reduction of the total longitudinal magnetization in the local image slice. This implies that an adequate delay time has to be introduced between the labeling and imaging data acquisition so that the labeled spins can reach the perfused tissues while remaining an inversed longitudinal magnetization. The data acquisition is typically accomplished with a single-shot technique, such as the echo planar imaging (EPI) (Mansfield, 1977), to achieve sufficient SNR. In order to reduce the complication from the so-called magnetic transfer effect (MT), the same labeling RF field is also applied during the acquisition of the control image, except that the field gradient is different. This is the basic setup of a CASL experiment. More complicated schemes, such as double inversion, can also be used to improve the labeling efficiency while minimizing MT effects (Alsop & Detre, 1998). The main concerns of the CASL techniques are the use of a separate labeling surface coil and the specific absorption rate (SAR) associated with the relatively long labeling period.

In PASL a relative short adiabatic inversion RF pulse (in the order of 10 ms) is commonly used to label the magnetization of the proton spins in the arterial blood, even though saturation pulses were also used in the earlier versions of the PASL method. The implementation of the PASL method is typically accomplished by using the imaging coil without the need of a separate labeling surface coil. Several different versions of PASL have been developed in order to increase the labeling efficiency or improve the accuracy for quantification by taking advantage of geometry differences of the inversion volume. The PASL pulse sequences can be divided into two main categories where the labeling is applied symmetrically or asymmetrically to the imaging volume (Golay et al., 2004). One major limitation of the early versions of PASL is the possibility to achieve an absolute quantification of the regional cerebral perfusion. This is partly limited by the time that is needed for the labeled arterial blood spins to flow from the labeling plane into the capillary bed of the image slices. This time may vary for the different sequential imaging slices. This effect can become problematic for perfusion quantification in some PASL pulse sequences, for example, the flow-sensitive alternating inversion recovery (FAIR) pulse sequence. In order to improve the labeling efficiency and quantification accuracy of the FAIR technique, more sophisticated labeling schemes based on the basic idea of the FAIR pulse sequence have been introduced in the past (Wong, Buxton, & Frank, 1997, 1998a, 1998b).

There are drawbacks of the early ASL techniques including compromised SNR or labeling efficiency and poor temporal resolution associated with the use of long labeling RF-pulses and subtraction of labeled and control images. To increase the temporal and spatial resolution the pseudo-continuous version of PASL was invented with the potential of combining the advantages with CASL and PASL and therefore providing a better balance between labeling efficiency and SNR (Detre, Leigh, Williams, & Koretsky, 1992; Silva & Kim, 1999; Wu, Fernández-Seara, Detre, Wehrli, & Wang, 2007). In order to obtain accurate perfusion quantification with high labeling efficiency it is desired that the labeling pulse should fully invert the magnetization to induce a label, while the pulse used for the control scan should not perturb the equivalent magnetization at all (Frank, Wong, & Buxton, 1997). It has previously been demonstrated that CASL provides more efficient spin labeling and higher signal yield compared to PASL in theoretical and experimental studies (Nezamzadeh, Matson, Young, Weiner, & Schuff, 2010). However, the advantage of CASL is offset by a range of technical complications as outlined above. In pCASL, the continuous labeling is achieved by a train of rapidly repeating, low flip angle, slice-selective RF pulses in combination with alternating bipolar magnetic field gradient pulses. During labeling the gradient pulses should have a small but non-zero value, during the control condition the phase of every second RF-pulse is shifted compared to the label condition and the mean gradient amplitude should be zero (Alsop et al., 2015). Pseudo continuous ASL can be implemented without the need of continuous RF capability and can even achieve better compensation of adverse MT effects than CASL. It has been shown by theoretical computations and experimental studies that the labeling efficiency in pCASL depends on the flow velocity and an adequate design of the RF and gradient pulse waveforms are important to achieve an optimal labeling efficiency (Jahanian, Noll, & Hernandez-Garcia, 2011). Furthermore, the labeling efficiency can be compromised by the off-resonance effect associated with the B_0 inhomogeneity at the labeling location. Therefore, it is necessary to implement robust calibration techniques for pCASL measurements, especially at ultra-high magnetic fields such as 7T (Luh, Talagala, Li, & Bandettini, 2013). In summary, the pCASL pulse sequence allows for whole brain coverage by taking advantage of the higher SNR from CASL without the use of a local RF-coil (Dai, Garcia, de Bazelaire, & Alsop, 2008; Luh et al., 2013; Wu et al., 2007). A schematic overview of the pCASL pulse sequence is shown in figure 3.

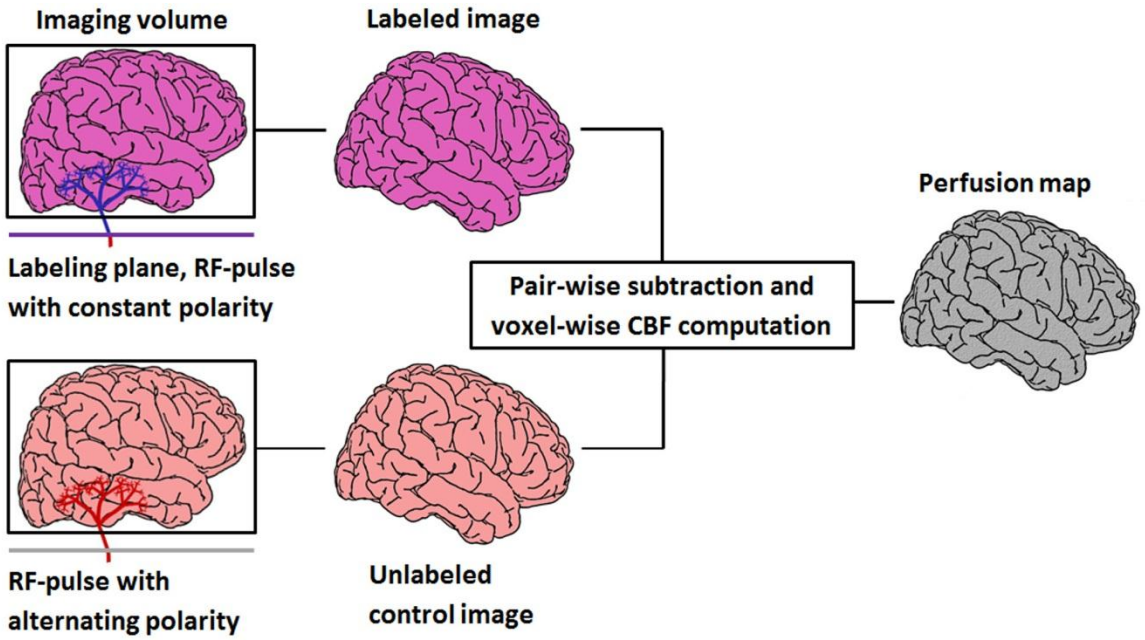

Figure 3 Acquisition and pair-wise subtraction of labeled- and control images acquired with pCASL are followed by CBF computation, resulting in a perfusion map of the brain.

1.3.2 Resting-state BOLD

The BOLD fMRI technique, which was first proposed by Ogawa in 1990, uses signal differences in oxygenated- and deoxygenated blood to map the activity of the brain (Ogawa, Lee, Kay, & Tank, 1990). When neurons in the brain are active they consume oxygen as a part of their metabolic process. This oxygen consumption is over-compensated by an excessive increase in oxygenated blood that can be measured as an increase in BOLD signal following the diamagnetic properties of oxygenated blood in relation to the paramagnetic properties of deoxygenated blood (Buxton, Wong, & Frank, 1998; Raichle, Grubb, Gado, Eichling, & Ter-Pogossian, 1976). Images with strong BOLD-contrast are generally acquired using T2*-weighted EPI sequences that can be repeated dynamically with a temporal resolution in the order of 1 second and whole brain coverage. After preprocessing of BOLD fMRI image data the analysis is set out to find spatiotemporal correlations with functional activities in the brain. Functionally relevant signals in BOLD fMRI data acquired during resting-state were first found by Biswal et al. in 1995 during efforts to remove physiological artifacts, such as respiratory and cardiac fluctuations, in BOLD fMRI data (Biswal, Yetkin, Haughton, & Hyde, 1995). This finding has led to the fast growing research field of brain functional connectivity mapping, exploring the activities of the resting brain. During resting-state fMRI measurements the participating subject is usually instructed not to think about anything special. The examinations are preferably carried out in a dark room, the subject might be instructed to focus their sight on some type of crosshair in order to stay awake and avoid eye movements. The temporal correlations in slow fluctuations of the BOLD signal in different brain regions are often referred to as brain functional connectivity. Research on the resting-state functional connectivity has become a useful tool for neuroscience research and is widely used to study the functional networks in both normal and diseased brains (Lowe, 2010).

1.3.3 ASL vs. BOLD

Both ASL and BOLD fMRI techniques are used to study the human brain during activation and at rest. There are some fundamental differences between the two techniques. While BOLD measures the increase of oxygenated blood as an indirect effect following a neuronal activation, ASL measures directly the regional cerebral blood flow (rCBF) changes. Previous studies have shown that BOLD fMRI has higher SNR and statistical power for experimental designs within subjects. However, the baseline drift in BOLD fMRI measurements can be problematic and hamper the possibility to detect slow variations in neural activity, ASL performs better for within subject experimental designs studying these slow changes ($\leq$0.009Hz) in neural activity because the drift effects are minimized by the pairwise subtraction of labeled and control scans. This pairwise subtraction also results in less problems with physiological artifacts (J. Wang et al., 2003). ASL also provides higher sensitivity to longitudinal studies across populations of subjects (Aguirre, Detre, Zarahn, & Alsop, 2002; Detre & Wang, 2002). In summary, the BOLD technique has high SNR and temporal resolution and is well suited for event-related fMRI studies. ASL provides the possibility to study the hemodynamic response directly since it is quantifiable. ASL is suitable for studying slow neural changes and longitudinal study designs. Both techniques can be used to study the resting-state functional connectivity.

1.4 ANALYSIS OF FMRI DATA

The acquired raw-data should always be checked for image quality. This can be performed by a visual inspection so that possible major image artifacts can be detected and the defected image series can be excluded. Examples of such artifacts include motion artifacts, RF-interference and spikes in the raw data. Following the initial quality control preprocessing should be performed, aiming at reducing known confounders and thereby increasing SNR. Some preprocessing steps for the imaging data from ASL and BOLD fMRI measurements are similar. The main steps include motion correction, creation of a brain mask to remove non-brain tissue, registration to a standard brain template and spatial smoothing to increase SNR. For BOLD fMRI data some further preprocessing procedures are necessary, such as slice timing correction for 2D acquisitions and physiological noise reduction. More details on this can be found in a recent review article on the topic (J. E. Chen & Glover, 2015). Before entering further statistical analysis a second inspection of the image quality should be performed to make sure all preprocessing steps have been carried out correctly. The motion correction can be controlled by looking at 1D-curves displaying the motion in each direction, all brains in the study should also be correctly aligned to the standard template and all non-brain tissue should be removed without the loss of any brain tissue. The modeling and statistical analysis following preprocessing differs between the different techniques and depending on the study design and available auxiliary data. Brief descriptions of the analysis methods that have been used or tested in the studies presented in this thesis are given in the following sections.

1.4.1 CBF computation

ASL data has a relatively low SNR and the perfusion signal is limited to 1-5% of the mean signal intensity in the images, mainly because of the relatively small volume fraction of cerebral flow in the brain tissue. The effect of T1 decay of the proton spins in arterial blood during the transit time from labeling to the imaging acquisition further diminishes the detectable signal. Motion correction is a critical preprocessing step because motion between the label- and control scans may give rise to inaccurate CBF values. Other critical preprocessing steps are spatial smoothing and normalizing which can cause an over- or under estimation of CBF if they are not adequately performed. It is very important that the preprocessing steps are performed correctly in order to not lose any information (Z. Wang, Aguirre, et al., 2008). After the initial preprocessing steps pair-wise subtraction is performed between the control and labeled images. Voxel-wise CBF computation can be performed using a calibration factor according to equation 14 as described by Wang et al. in 2008:

(14)
$$CBF = \frac{\Delta M \lambda R_{1a} e^{\omega R_{1a}}}{2 M_0 \alpha} [1 - e^{-\tau R_{1a}}]^{-1}$$

where ΔM is the signal difference from the pair-wise image subtraction, R_{1a} is the longitudinal relaxation rate of blood, τ is the labeling time, ω is the post labeling delay time, α is the labeling efficiency, λ is the blood/tissue water partition coefficient and M_0 is approximated by the control image intensity. The result from this equation is an absolute CBF map of the imaged slice or volume. Inter-subject variations in global CBF associated with non-neural factors such as breathing pattern, physiologic state and caffeine consumption contributes to noise in group comparisons. In order to increase the statistical power to detect the true group differences in regional CBF these factors can be reduced by using spatial voxel-wise normalization (Aslan & Lu, 2010).

1.4.2 Seed-based analysis

Seed-based analysis of resting-state BOLD fMRI data is a frequently used analysis method that requires some a priori knowledge about the data (Biswal et al., 1995; Cordes et al., 2000). The temporal fluctuations of the BOLD fMRI signal from a seed region or voxel are extracted and used as a reference time course to find synchronous activity in the rest of the brain by correlation analysis (Bandettini, Jesmanowicz, Wong, & Hyde, 1993) or general linear modeling (GLM) (Friston et al., 1995). Functional connectivity patterns associated with the seed time course can then be compared between different groups, for example patients and normal controls. The selection of the seed can, therefore, introduce bias for the functional connectivity networks to be studied. If there is no sufficient prior knowledge or hypothesis to guide the selection of the seed region, the rCBF results from ASL measurements can provide very useful guidelines. For example, a brain region exhibiting large rCBF variations may imply that it is a network node with central functional connectivity.

1.4.3 ICA analysis

ICA (independent component analysis) is a general signal processing method for separating multivariate signal into its sub components. It is a data driven method that is often used to analyze BOLD fMRI data, especially useful for task-free, resting-state fMRI data (Calhoun, Adali, Pearlson, & Pekar, 2001; McKeown & Sejnowski, 1998). In ICA the brain imaging data are represented by a predefined number of components that are assumed to be statistically independent of each other. The average time course for each component is used to create activation maps corresponding to the signal source by using higher order statistical criteria. The ICA method has its limitations. First of all, its results are dependent on how many components the user chooses to include into the analysis, which in turn affects the appearance of the activation maps (Y. Wang & Li, 2015). Secondly, it is up to interpretation which components are noise and which are true signal (J. E. Chen & Glover, 2015).

1.4.4 Quantitative data-driven analysis

Quantitative data-driven analysis (QDA) is a newly developed method useful for the analysis of resting-state fMRI data without any a priori knowledge or hypothesis. Using this method two metrics are derived: CCI (connection count index) and CSI (connection strength index). The indices can be used for direct comparison of functional connectivity measurements between different subjects and at different time points (T. Q. Li, Hallin, & Juto, 2015; Nordin et al., 2016). With QDA the Pearson's cross-correlation coefficients (CC) for the time course of each voxel of the brain imaging data in relation to all other voxels in the brain are computed. The correlation matrix is used to derive the CCI and CSI metrics. The CSI is defined as the non-zero mean value of the cross-correlation coefficients between a given voxel and all other voxels above a certain threshold. The CCI is the number of voxel pairs that each voxel connects to with a cross-correlation above a given threshold. The selection of the correlation coefficient threshold is preferably implemented so that the functional connectivity results are statistically significant and stable. We have carefully investigated this point (Nordin et al., 2016) by systematically comparing the statistical results under different threshold values.

1.4.5 Statistical analysis

In order to further analyze the results from fMRI studies there are several statistical tools available. In order to interpret the results correctly it is important to use validated statistical methods (Eklund, Nichols, & Knutsson, 2016). For the studies presented in this current thesis tools from AFNI (http://afni.nimh.nih.gov/afni) and FSL (http://www.fmrib.ox.ac.uk/fsl) have been used. FSL provides the possibility to specify temporal study design- as well as corresponding contrast matrices used to perform post-hoc regression analysis of the data. This post-hoc regression analysis is incorporated in the FSL-tool MELODIC. AFNI provides separate tools for statistical voxel-wise analysis of 3D data sets, such as 3dANOVA3 for three-factor ANOVA, 3dRegAna for multiple linear regression analysis and 3dttest for comparing the means of two data sets. To study the effect between two independent groups t-test or regression analysis can be used. In 3dRegAna other factors can also be included, such

as a measured variable from an fMRI paradigm or intervention. To study the change over time within a group of subjects it is preferable to use ANOVA analysis to avoid problems with independence. The program 3dANOVA3 can be used to study the effect of multiple factors, such as changes over time (e.g. fMRI measurements at different time points after an intervention) and group differences (e.g. patients and normal controls). The most interesting feature is that it also provides an analysis of the interaction effect between the main factors. The study design and the type of data to be analyzed determine what tool to use and the implementation. When accessing the statistical significance of the results from voxel-wise statistical tests, a voxel-wise threshold in combination with a minimum cluster size are commonly implemented. One way of determining an adequate cluster size is to use the AFNI program *3dClustSim* that performs Monte-Carlo simulations to estimate the probability of false positive clusters. In addition to an appropriate cluster size the desired voxel-wise p-value should be set to include only voxels with a certain probability of representing a true effect. Clusters with significant rCBF or BOLD fMRI signal changes can be subjected for further ROI analysis on the results. For example to decide the change over time on rCBF in response to an intervention, the significant clusters resulting from voxel-wise statistical analysis can be used to extract the mean rCBF at each time point from that specific cluster. The rCBF data may then be used for further regression analysis with any other desired parameter of interest for the intervention in any standard statistical software to further scrutinize the results. These analysis steps are vital to understand whether a detected effect is of true neural origin or simply false positive effects from random noise.

1.5 OVERVIEW OF THE INVESTIGATED DRUG AND CONDITION

The goal of this thesis was to use functional MRI techniques to study drug and disease effects on the human brain. We have used arterial spin labeling to monitor the effects of a central nervous system (CNS) active drug on the brain cerebral blood flow. We have also studied a patient group suffering from chronic fatigue following mild traumatic brain injury (mTBI) by using both ASL and resting-state BOLD fMRI. The choice of the CNS drug and background of the patient group are further explained in details in the following two sections.

1.5.1 Amphetamine

In order to investigate the effects of CNS active drugs by monitoring CBF changes after dose and to use the perfusion data to produce a pharmacokinetic/pharmacodynamic model for the CNS drug responses in the human brain, a CNS active drug with a well-known effect is appropriate. Many CNS active drugs have a dose dependent effect on neuronal activity (Ren, Xu, Choi, Jenkins, & Chen, 2009). Changes in regional cerebral blood flow (rCBF) following intake of a CNS active drug can reflect neuronal activity changes induced by the drug. In order to evaluate the ASL method, a CNS drug that is both available at the pharmacy, thorough tested and evaluated was sought, to meet these criteria, dextro (d)-amphetamine was chosen. Amphetamine has suitable biological half-life and absorption time to allow for comparison between rCBF changes and blood plasma concentration of the drug during a 10 hour period. Previous studies on amphetamine have shown dose-dependent activation

patterns related to the drugs specific interactions with the dopaminergic systems in animal models and human subjects (Bruns, Kunnecke, Risterucci, Moreau, & von Kienlin, 2009; Devous, Trivedi, & Rush, 2001; Price et al., 2002; Silva et al., 1995; Vollenweider, Maguire, Leenders, Mathys, & Angst, 1998). The subjects in the study presented later on in this thesis received either an oral dose of 20 mg d-amphetamine or placebo. This was considered to be a low dose, suitable for studies on healthy human subjects.

1.5.2 Mild traumatic brain injury

We have also investigated patients suffering from chronic fatigue following mild traumatic brain injury (mTBI) in order to detect possible functional connectivity abnormalities. The annual incidence of hospital-treated mTBI has been estimated to be 100 – 300 per 100.000 in the industrialized world and over 600 per 100,000 when including those who do not seek emergency medical care (Cassidy et al., 2004). The American Congress of Rehabilitation Medicine have established following criteria for mTBI: Traumatically induced physiological disruption of brain function as manifested by at least one of the following criteria: 1) Loss of consciousness up to 30 minutes; 2) Loss of memory within 24 hours from trauma; 3) Confusion or disorientation (Glasgow coma scale administered 30 minutes post injury between 13-15; 4) Other neurological abnormalities such as focal signs or intracranial lesion (not requiring surgery); 5) The signs of mTBI must not have any other explanation such as drug intoxication, psychological trauma etc. ("Mild Traumatic Brain Injury Committee of the Head Injury Interdisciplinary Special Interest Group of the American Congress of Rehabilitation Medicine: Definition of mild traumatic brain injury," 1993). Chronic fatigue is one of the most commonly reported and long-lasting post-concussion symptoms (Lannsjo, af Geijerstam, Johansson, Bring, & Borg, 2009). Enhanced sensitivity to effort and limited endurance for sustained physical and mental activities are the main characteristics of central fatigue (Chaudhuri & Behan, 2004). Fatigue is also associated with reduced social and physical functioning (Rosenthal, 2008; Stulemeijer et al., 2006). The pathological and physiological mechanisms behind chronic fatigue following mTBI are still not fully understood. A better understanding of these mechanisms would be of clinical importance in order to design rehabilitation programs or pharmacological treatments.

2 AIMS OF THIS THESIS

The overall aims of the studies included in this thesis are the following: 1) To assess the reproducibility and reliability of rCBF measurements conducted at 3T with the pCASL technique; 2) To study the pharmacokinetics of a CNS-active drug in normal volunteers by conducting rCBF measurements as a function of time after intake of d-amphetamine using the pCASL technique; 3) To investigate the possible neurological abnormalities of mTBI patients with chronic fatigue by performing rCBF and resting-sate functional connectivity measurements before, during and after a 20 minute continuous psychomotor vigilance task (PVT). In addition to the clinical diagnostic value these studies may provide, we also aim at contributing to important knowledge in the design and analysis of brain functional imaging studies. The specific aims of the included studies are the following:

Study I To characterize and optimize the reliability and accuracy of perfusion measurements by the pCASL technique at 3T using a test and re-test strategy, extensive experimental measurements in normal controls and complementary computer simulations.

Study II To quantify and model neurological response patterns measured by regional CBF changes in relation to variations in concentration of d-amphetamine in the blood plasma after intake of 20 mg d-amphetamine and to use the results from voxel-wise and ROI-based analyses to construct a pharmacokinetic/ pharmacodynamic model of the drug response.

Study III To detect possible abnormalities in the resting-state functional connectivity in mTBI patients suffering from chronic fatigue before and after the performance of a PVT measuring reaction time by comparing the results to a healthy control group using resting-state BOLD fMRI and quantitative data-driven analysis.

Study IV To study the CBF response and functional connectivity changes during a PVT measuring reaction time in mTBI patients suffering from chronic fatigue and compare the results to healthy controls using the pCASL technique and voxel-wise analysis of the normalized CBF-data.

3 MATERIALS AND METHODS

3.1 ETHICAL CONSIDERATIONS

The regional ethics committee in Stockholm approved study I (dnr: 2010/149-31/1 & 2010/1917-31/1), study II (dnr: 2009/2015-32), study III and IV (dnr. 2008/1458-31 & 2010/202-32) and they were all carried out in accordance with the approved guidelines. All participants received verbal and written information about the studies before signing an informed consent.

3.2 GENERAL PREPARATIONS AND FMRI

In the preparations and implementation of an fMRI experiment it is very important to take all precautionary steps possible to make sure the resulting data is of high quality. This includes quality assurance (QA) of the MRI equipment and preparing the subjects and the scanner. The quality controls performed during the studies presented in this thesis included SNR measurement on a homogenous phantom to make sure all coil elements were functioning appropriately, stability measurement over time for an EPI sequence, measurement of ghosting artifacts, stability and homogeneity of the magnetic field. These QA measurements were performed every second week. Before each scan during the studies the participants were instructed on how to behave in the scanner in order to keep motion to a minimum and get as good resting-state as well as behavioral data as possible. Each subject was positioned and fixated carefully in the head coil using foam padding. Before starting the examination the field of view was carefully positioned in order to cover as much as possible of the brain. Local shimming was performed to optimize the magnetic field surrounding the subject and thereby minimize local distortion and signal loss.

All the pCASL and BOLD fMRI measurements were performed on a Siemens Magnetom Trio 3T clinical MRI system (Siemens Medical Solution, Erlangen, Germany). The scanner was equipped with a 32-channel receive-only head coil. The pCASL data was acquired using a 2D single-shot EPI sequence. The BOLD data was acquired using a gradient-recalled echo 2D EPI sequence. The acquisition parameters for the fMRI sequences are described in table 2. The number of acquisitions depended upon implementation and will be specified in the following sections. For more detailed materials and methods the reader is referred to the full scientific papers.

Table 2 Sequence parameters for the pCASL and BOLD fMRI sequences used in study I-IV.

Sequence parameter	pCASL study I	pCASL study II & IV	Resting-state BOLD study II & III
Labeling duration	1600 ms	1600 ms	-
Post-labeling delay	1200 ms	1200 ms	-
TE/TR	18/3515 ms	18/3330 ms	35/2000 ms
FOV	220×220	230×230	204×204 mm
Matrix size	64×64	64×64	68×68
Slices	18	18	34
Slice thickness	6 mm	6 mm	3.5 mm
Inter slice gap	1 mm	0.6 mm	-
Band width	2600 Hz/px	2790 Hz/px	2626 Hz/px
Flip angle	90º	90º	90º
Parallel imaging	GRAPPA (iPAT 2)	GRAPPA (iPAT 2)	GRAPPA (iPAT 2)

3.2.1 Study I

This study included sixty-four normal adult volunteers (m/f=23/41, mean age 34±8 years, range 20-46), ten of the male subjects also volunteered for the intra-subject variability measurement including 7 or more pCASL scans with repositioning. All pCASL scans included 150 acquisitions with a total acquisition time of about 8 min.

The preprocessing of the pCASL data was performed using tools from the AFNI package, the main procedures included: 1) Motion correction; 2) Creation of brain mask; 3) Voxel-wise CBF computation; 4) Brain normalization to align individual CBF data to the T1-weighted Talairac brain template; 5) Creation of CBF template with 3×3×3 mm^3 spatial resolution based on the average of the registered CBF results for all subjects; 6) 2nd pass registration of the CBF results with the established CBF template; 7) Voxel-wise statistical analyses including the mean, standard deviation, coefficient variation (CV), minimum, and maximum; 8) Calculating the ROI average results from the statistical maps for 33 ROIs which were pooled from the ROIs defined in the Talairac template. In addition, a gray matter (GM) mask was created from the tissue prior template included in FSL software package. In order to estimate the true instrumental error in CBF measurements random permutation computations were performed for the pCASL raw data. Two data sets acquired without repositioning, resulting in totally 140 image pairs were randomly separated into 2 sections containing 70 image pairs each. This was repeated 400 times and the results analyzed in the same way as the rest of the data.

3.2.2 Study II

In study II 12 healthy normal male subjects were included (mean age 25 years, range 20-31). Each subject underwent a screening including a health- and clinical MRI examination within

30 days prior to the study participation. The subjects were fasting from midnight before MRI. Six of the subjects were randomly selected to receive a single oral dose of 20 mg d-amphetamine and six were given placebo. After intake of d-amphetamine or placebo pCASL data was acquired regularly during a 10 hours period according to table 3.

Table 3 The experimental design including the time points for MRI acquisitions, PK sampling, dose, vital signs and meals for each subject.

Event time (min)	MP-RAGE	Dose	ASL MRI	Resting-state BOLD	BP	PK sampling	Respiratory frequency	Meal
Pre dose	x		x	x	x	x	x	
0		x						
15			x		x	x	x	
30			x		x	x	x	
60			x		x	x	x	x
120			x	x	x	x	x	
180			x		x	x	x	
240			x		x	x	x	x
360			x		x	x	x	
480			x		x	x	x	x
600			x	x	x	x	x	

The scanning protocol included MPRAGE, resting-state functional MRI and pCASL perfusion measurement. For the pCASL scans 150 acquisitions were made before dose and 300 acquisitions after dose. The subjects were repositioned to match the initial head position after each pause from the scanning procedure. Before each pCASL scan blood samples and blood pressure were collected and during the MRI scans the pulse rate and respiratory rate were collected. The results from the blood samples were used to determine pharmacological parameters such as the maximal blood plasma concentration, the time of maximum plasma concentration and the terminal half-life of d-amphetamine.

The preprocessing of the pCASL data was performed using tools from the AFNI package, the main procedures included: 1) Motion correction; 2) Creation of brain mask; 3) Voxel-wise CBF computation; 4) Brain normalization to align individual CBF data to the T1-weighted Talairac brain template. To identify the overall response difference between subjects receiving d-amphetamine or placebo, voxel-wise student t-test was performed. Voxel-wise regression analysis was carried out to depict the brain regions with significant drug response. The regression analysis was performed using the AFNI program, 3dRegAna. Finally a 3-way ANOVA was used to analyze the effects of group, time and the interaction effect of group and time using the AFNI tool 3dANOVA3.

The average whole-brain GM CBF and plasma concentrations of d-amphetamine were analyzed individually using pharmacokinetic/pharmacodynamic modeling.

3.2.3 Study III-IV

Both pCASL and resting-state BOLD fMRI techniques were used for the study of mTBI patients. For clarity of the presentation, the results from the mTBI study were separated into parts, which facilitate also the analysis and interpretation.

Ten mild traumatic brain injury (mTBI) patients (m/f 5/5) and 10 healthy controls (m/f 5/5) were recruited to the study. The mean age of the patients was 37.5 years (range 20-52 years, SD 11.2) and the mean educational length was 13.1 years (SD 1.6). The healthy controls were matched for age, gender and years of education with a mean age of 36.9 years (range 20-47 years, SD 11.0) and the mean educational length was 13.4 years (SD 2.0).

Self-rated general fatigue was measured with the fatigue severity scale (FSS). The self-rated current fatigue level was assessed using a visual analog scale of fatigue (VAS-f). The VAS-f ranges from 0 corresponding to no fatigue, to 10 corresponding to the worst possible fatigue. Sleep quality was measured with a Swedish version of the Pittsburgh Sleep Quality Index (PSQI). Medications, tobacco, coffee and tea consumptions, food and fluid intakes and the number of hours of sleep were recorded for each participant on the study day.

The MRI data acquisition protocol included the following scanning sessions: (1) 3-plane localizer; (2) Conventional clinical MRI scans including 3D T1-weighted MPRAGE, SWI, FLAIR, T2-weighted GRE and DWI; (3) The 1^{st} session of 8-minute long resting-state BOLD fMRI with 240 dynamic timeframes; (4) A 8 minute long pCASL acquisition containing 150 measurements during resting-state conditions; (5) A 20-minute long psychomotor vigilance task (PVT) with simultaneous pCASL acquisition containing 400 measurements; (6) The 2^{nd} session of 8-min long resting-state BOLD fMRI with 240 dynamic timeframes. The setup for the PVT included a projector-based visual system with feedback to measure the reaction times (RT) of the participants. The stimulus paradigm was created in E-Prime software (Psychology Software Tools Inc., Pittsburgh, PA). The participants were instructed to press a response button as quickly as they could when a set of zeroes appeared on the screen. The paradigm also included false starts, when the participants were instructed not to press the response button when numbers appeared on the screen.

Preprocessing of the resting-state fMRI data included removal of the first timeframes in each data set to ensure signal steady state. Motion correction and temporal de-spiking was performed. The average volume for each time series was used to generate a brain mask to minimize the amount of extra-cerebral tissues. Spatial normalization to the standard MNI template was performed. The imaging data was re-sampled to isotropic resolution by using a Gaussian kernel. Removal of nuisance signal was performed by voxel-wise regression. Baseline trend removal was performed followed by effective band-pass filtering using low-pass filtering at 0.08 Hz. Finally local Gaussian smoothing was performed. These preprocessing steps were executed using tools from FSL and AFNI.

The preprocessing of the pCASL data was performed using tools from the AFNI package, the main procedures included: 1) Motion correction; 2) Creation of brain mask; 3) Voxel-wise CBF computation; 4) Brain normalization to align individual CBF data to the T1-weighted Talairac brain template. The 20 min long pCASL sequence was divided into five 4 min quintiles in order to study the effect of time during the PVT.

Quantitative data driven analysis was used to compute CSI and CCI from the resting-state fMRI data. For comparison of the functional connectivity (CCI and CSI) results between mTBI patients and healthy controls measured before and after the PVT, we performed voxel-wise 3-way analysis of variance (ANOVA) using the AFNI program 3dANOVA3. The group difference between mTBI patients and healthy controls and temporal difference before and after the PVT were modeled as fixed factors. The participants in each group were modeled as a random factor. With 3-way ANOVA, we can also assess the interaction between the 2 fixed factors and investigate how the continuous PVT performance affected the functional connectivity in mTBI patients and healthy controls. To study the correlation between fatigue and brain functional connectivity derived from resting-state fMRI measurements, voxel-wise linear regression analysis was performed with the CSI and CCI image data using the AFNI program, 3dRegAna. To gain sufficient statistical power, the data for all participants acquired before and after the PVT task were first pooled together for the regression analysis. Further regression analyses were also performed for each group separately.

The CBF data calculated from the pCASL sequences was analyzed using a 3-way ANOVA (AFNI, 3dANOVA3), regression analysis (AFNI, 3dRegAna) and t-tests (AFNI, 3dttest). The CBF from the PVT was normalized voxel-wise to each individual's mean CBF during resting-state conditions. The main factors of the ANOVA included the time effect in order to detect CBF changes between the 5 quintiles of the PVT and group to study differences between patients and healthy controls during the PVT. The subjects were considered as a random factor. Regression analysis was performed to analyze the effects of measured reaction time and the estimated level of fatigue, VAS-f, on CBF during PVT. Group CBF differences during resting-state conditions and during the PVT was analyzed using t-tests.

4 RESULTS AND DISCUSSION STUDY I-IV

In the following sections a summary of the results followed by a brief discussion is given for each of the studies included in this thesis. For more detailed results and discussions the reader is referred to the full scientific papers.

4.1 RESULTS STUDY I

In study I we have investigated and evaluated the inter- and intra-subject variability of CBF measurements using a pCASL protocol.

The voxel-wise statistical results from the intra-subject variability study show that the cerebrospinal fluid (CSF) and GM have higher standard deviations compared to white matter (WM). The brain boundary (CSF space) and WM regions show the highest coefficient of variation (CV). The corresponding results for CBF measurements in all 64 participants shows that the standard deviation and CV depicted similar spatial distribution patterns as those for the intra-subject results but with increased magnitudes. Histograms for the inter-subject averaged regional CBF images and CV data are shown in figure 4 a) and b) respectively.

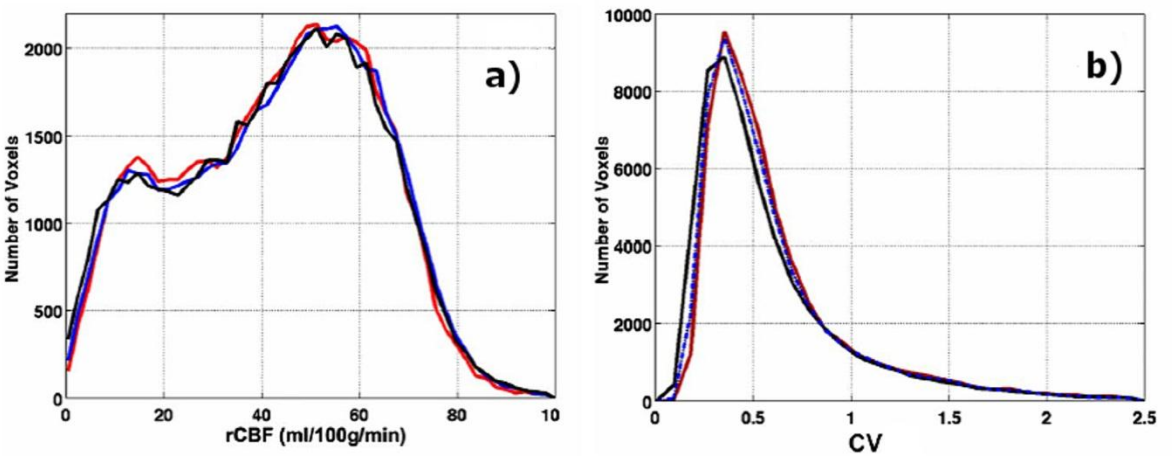

Figure 4 Histograms for the inter-subject averaged regional CBF data (a) and the corresponding CV (b). The black curve is based on 20 subjects, the red curve is based on 40 subjects and the blue curve is based on 64 subjects.

The CV and CBF histograms based 40 and 60 data sets showed minor differences, indicating that the average results of the measured data is approaching steady state at N>40.

Analysis of scatter plots of the voxel-wise CV versus CBF for the inter-subject and intra-subject averaged data show that the inter-subject averaged results indicate a nearly inverse relationship between CV and CBF, whereas the intra-subject averaged results depict a relatively constant CV until reaching the lower end of CBF <10 ml/100g/min. Overall, the inter-subject results show much higher CV level than that for the intra-subject averaged data as shown in figure 5.

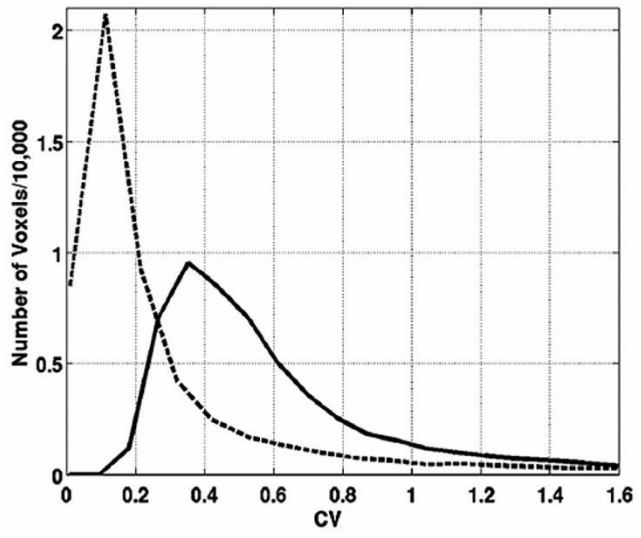

Figure 5 Histograms of CV for the inter-subject (solid line) and intra-subject (dashed line) averaged data.

The average CBF in GM measured by the pCASL method in the 64 participants is 52.02±24.46 ml/100g/min. For voxels in the GM region, the average CV estimated from the inter-subject CBF results is 52%, whereas the average CV estimated from the intra-subject CBF results is 31%. The statistical results for the different ROIs showed substantial heterogeneity. The cingulate cortices (anterior, middle, and posterior) are among the brain regions with the highest CBF. The basal ganglia nuclei, such as caudate and pallidum, have the lowest CBF. Most ROIs on the left hemisphere showed higher CBF (average=11%, range 4-35%) compared to the corresponding ROIs on the right hemisphere except for insular lobe, caudate, and pallidum.

The variability of the simulated results based on two successive pCASL measurements is quite close to that for the intra-subject multi-session rCBF measurements.

4.2 DISCUSSION STUDY I

The amount of pCASL data included in study I have enabled robust statistical analyses to be performed both voxel-wise and in standard ROIs. The results show that the rCBF data based on ROIs demonstrated good repeatability, the CV for multi-session intra-subject data was 5-9% depending on the time interval between sessions and the CV for the inter-subject rCBF data was 20%. These results are consistent with the findings reported in previous ASL repeatability studies which were largely based on ROI analysis (Parkes, Rashid, Chard, & Tofts, 2004). In another study results from three different pulsed ASL techniques were compared and it was reported that the CV was less than 9% for both GM and WM when intra-subject measurements were conducted within two hours (Jahng et al., 2005). Other ASL studies with complementary ^{15}O-water PET results reported a variation of 8% in WM and 10% in GM for measurements performed within 2-day intervals, these reported literature results were based on rCBF data with substantial spatial smoothing (Carroll et al., 2002; Xu et al., 2010).

The most interesting findings in study I are that the voxel-wise rCBF values showed substantially higher variability both for the inter-subject (50% variation) and intra-subject (30% variation) data sets. The large variability in the voxel-based rCBF data implicates that it is difficult to reliably detect response from a single voxel or small cluster of voxels in functional activation and pharmacokinetic studies with the pCASL technique.

The sources of variability in pCASL perfusion measurements are generally of technical or physiological natures. Comparing the results from the inter-subject, intra-subject, and permutation simulations can give us important insight into the origins of the variability. The variability difference between the multi-session intra-subject rCBF data and the simulation results based on two successive measurements is approximately 5%. This is likely the error due to physiological changes during scans and repositioning effects, meaning that the intra-subject variability of the CBF measurement is largely of technical origin. The large difference in variability between the voxel-wise and ROI-based rCBF data suggests that the instrumental error is mainly of SNR nature. With ROI averaging or spatial smoothing, the SNR of the CBF data can be improved at the cost of spatial resolution.

Although the measured mean perfusion values fall within the expected range, as measured by a variety of techniques (Bangen et al., 2009; Kastrup, Li, Glover, Kruger, & Moseley, 1999; Parkes et al., 2004; Xu et al., 2010; Ye et al., 2000b), the individual difference is large. The difference in variability between the inter- and intra-subject CBF measurements suggests its apparent physiological nature. The physiological effects can be divided into pure physiological differences, such as the level of basal blood flow, metabolism, age, gender and physiological differences which affect the labeling efficiency such as arterial transit time, relaxation rate of the blood and the arterial angle to the labeling plane.

The cause of the individual difference in rCBF might be linked to individual variation in metabolism, neuronal density and neuron number, which have been found to have a similarly large inter-subject variability (Henderson, Tomlinson, & Gibson, 1980; Pakkenberg & Gundersen, 1997). The human brain has a large capacity for perfusion change in response to external stimuli, arousal, pharmaceutical intake, and changes in awareness. In particular, the arterial concentration of CO2 appears to have a large effect on perfusion (T. Q. Li et al., 2000; T. Q. Li, Kastrup, Takahashi, & Moseley, 1999; T. Q. Li, Moseley, & Glover, 1999; Z. J. Li et al., 2004). A large part of the inter-subject variability in CBF can probably be explained by age- and gender effects. Reduction of CBF with aging has been extensively studied (Bangen et al., 2009; Biagi et al., 2007; Parkes et al., 2004; Restom, Bangen, Bondi, Perthen, & Liu, 2007; Xu et al., 2010). Gender differences in whole-brain perfusion with a higher CBF among females has been shown in a number of studies (Hogarth, Mackintosh, & Mary, 2007; Kastrup, Li, Glover, Kruger, et al., 1999; Parkes et al., 2004; J. Wang et al., 2007; Xu et al., 2010). The acquired data from study I was not sufficient to investigate age- or gender related effects adequately.

It has previously been shown that the pCASL inversion pulse labeling efficacy varies due to its sensitivity to blood velocity (Xu et al., 2010; Ye et al., 2000a). The label and control

conditions of the flowing arterial blood are defined by the specification of the phases in the labeling RF pulse train for pCASL. Therefore, the labeling efficiency is sensitive to flow velocity and off-resonance effects. The individual difference in the structure of the arteries, such as size and curvature in relation to the location of the labeling plane, can also influence the labeling efficiency. Additional calibration scans for each individual would improve the labeling efficiency.

4.3 RESULTS STUDY II

In study II we have investigated whether the pCASL technique is sufficiently robust to differentiate the hemodynamic response between two groups receiving either placebo or d-amphetamine.

From the physiological data the only significant difference found between the two groups was an increase of the systolic- and diastolic blood pressure for the d-amphetamine group compared to the placebo group. The pharmacokinetic results provide the mean time of the maximum plasma concentration of d-amphetamine, 3.2 hours after dose, and the mean terminal half-life was estimated to 11.8 hours.

The MRI results show significant group differences in temporal response to the dose in brain regions including the prefrontal cortex, basal ganglia, cingulate and insular cortex as a result of the ANOVA test. A significant interaction effect between group and time was also seen revealing that the dynamic CBF change was a combined effect of dose and time. A significant reduction of whole-brain GM CBF was seen at 3, 4 and 6 h after dose compared to placebo. The most significant change in CBF could be seen in the basal ganglia, frontal- and insular cortex. The patterns of CBF reduction for the subjects receiving d-amphetamine compared to placebo at different time points after dose are shown in figure 6. The measured CBF time course together with the predicted CBF time course from the pharmacokinetic/pharmacodynamic model is shown for each individual in figure 7.

A variation of the regional CBF response in relationship to the plasma concentration of d-amphetamine was found in different brain regions from the voxel-based regression analysis.

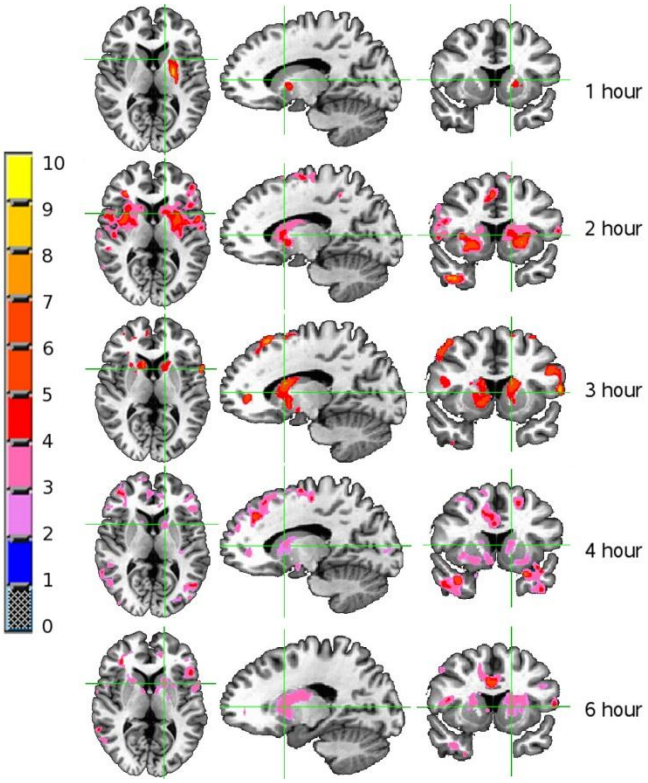

Figure 6 CBF response patterns to d-amphetamine intake compared to placebo at different time points after dose. Voxel-wise student t-test was used to find the brain regions with a significant CBF reduction.

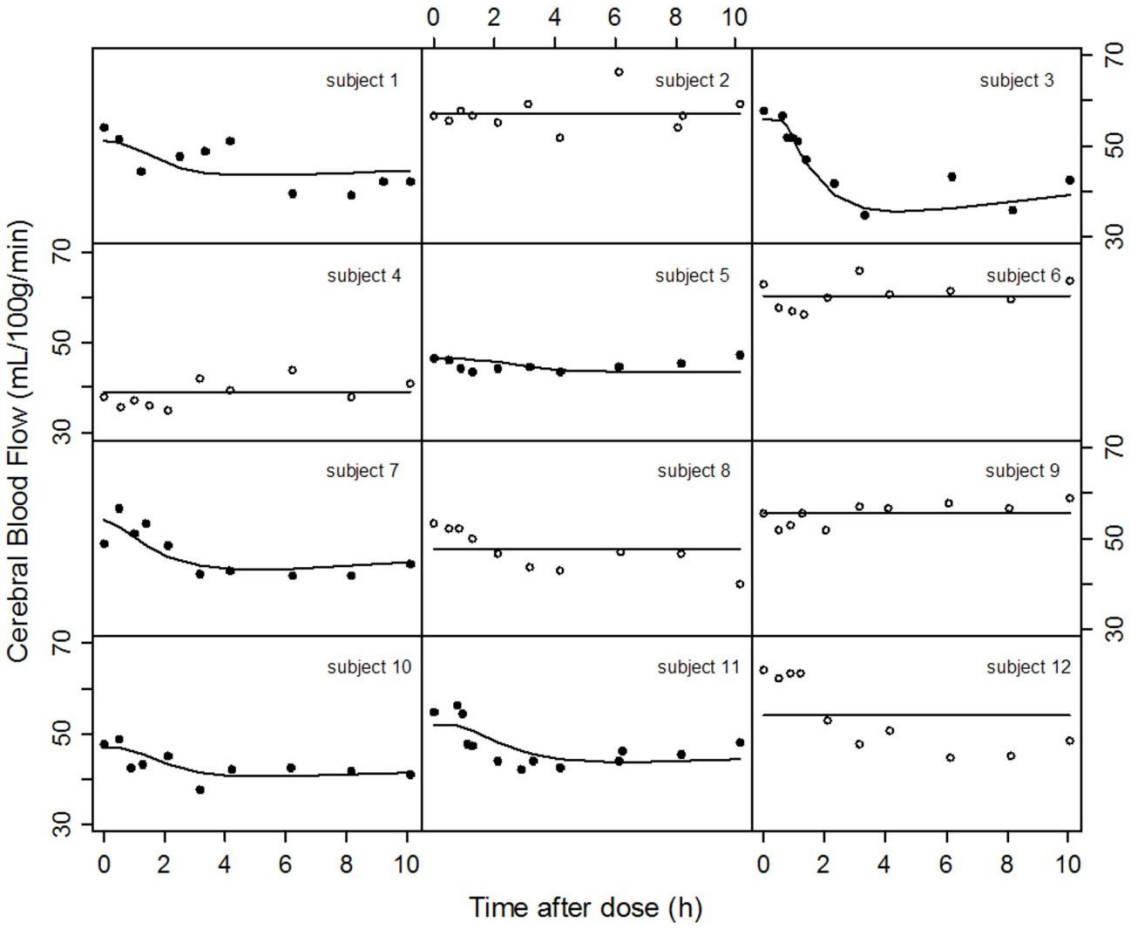

Figure 7 The measured (dots) and predicted (lines) CBF results for each subject. The solid dots represent the d-amphetamine group and empty dots the placebo group. The individual CBF prediction was produced by the pharmacokinetic/pharmacodynamic model.

4.4 DISCUSSION STUDY II

The results from study II revealed a significant decrease of whole brain GM CBF following the intake of d-amphetamine compared to placebo. These results correspond to findings in previous human studies (Kahn, Prohovnik, Lucas, & Sackeim, 1989; Mathew & Wilson, 1985; Wolkin et al., 1987). A dose dependent activation pattern has previously been shown in rats given 0.3 – 3 mg/kg (Bruns et al., 2009). In other studies an increase in CBF has been shown for baboons and rats after injection of 0.6–20 mg amphetamine/kg (Price et al., 2002; Silva et al., 1995). However the anesthesia used in many animal studies may affect the global CBF. In this current study 20 mg d-amphetamine was used which corresponds to approximately 0.26 mg/kg. In many animal studies the amphetamine dose is substantially higher. In a previous human study, both increases and decreases of rCBF have been reported for different brain regions after an amphetamine dose 0.4 mg/kg (Devous et al., 2001). CBF increase has previously been shown in humans following an amphetamine dose of 0.9-1.0 mg/kg studied by PET (Vollenweider et al., 1998). These results are probably explained by the dose dependent effect of amphetamine where an increase of CBF can be seen at high doses and a decrease of CBF at low doses. A CBF increase after 20 mg amphetamine intake in humans has been shown in a previous study based on dynamic susceptibility contrast MRI (Rose et al., 2006). Dynamic susceptibility contrast MRI provides relative CBF measurements and requires an external contrast agent to be administered to the subject. Successive injections of a contrast agent may change the measurement sensitivity which needs to be calibrated for quantitative comparisons (T. Q. Li et al., 2000). Regional or whole brain CBF changes in the range of 10-20% have previously been shown using ASL following administration of different CNS active drugs such as citalopram (Y. Chen et al., 2011), ecstasy (Schouw et al., 2011), caffeine (Grichisch et al., 2012), morphine and alcohol (Khalili-Mahani et al., 2011).

The mean blood pressure was within the normal range for the d-amphetamine and placebo groups, despite of the significant increase in systolic- and diastolic blood pressure that we could see. A constant perfusion is maintained for normal blood pressure changes because of the auto regulation of cerebral vasculature (Paulson, Strandgaard, & Edvinsson, 1990), therefore no normalization was performed to the blood pressure changes.

The results from study II show that the pCASL technique is sensitive enough to detect the CBF changes occurring after exposure to 20 mg d-amphetamine compared to placebo in a relatively small group of subjects. Pseudocontinuous ASL is a useful technique for pharmacokinetic/pharmacodynamic modeling of CNS active drugs. The acquired data from study II allows for comparison of pharmacokinetic/pharmacodynamic models over time. An accurate pharmacokinetic/pharmacodynamic model is important to assess the efficacy of CNS-active drugs and may serve as a bridging tool between preclinical and clinical research.

4.5 RESULTS STUDY III

In study 3 we have examined brain functional connectivity changes for post mTBI fatigue patients compared to healthy controls before and after a PVT measuring reaction time.

The mTBI patients reported significant higher general fatigue on the fatigue severity scale compared to the healthy controls. There was no significant difference between patients and controls regarding self-rated sleep quality or tea and coffee consumption before the MRI investigation. The body mass index (BMI) was approximately the same for the two groups.

There was no significant difference in self-rated current fatigue (VAS-f) between patients and controls before MRI scanning, but directly after the PVT performance the patients scored significantly higher for current fatigue compared to the controls. The mTBI patients displayed significantly longer mean reaction time and higher standard deviation in the reaction time compared to the controls.

The results obtained from the 3-way ANOVA of the functional connectivity indices data (CCI and CSI) can be seen in figure 8.

As detailed in table 4, PVT induced CCI and CSI increase in a number of functional networks involving both motor-sensory, attention and executive control. Significant differences in CCI and CSI between mTBI patients and healthy controls were found in thalamus and medial frontal gyri, respectively.

The CCI and CSI in the dorsal anterior cingulate depict significant interaction effects between group and time. The PVT affects the functional connectivity of the mTBI patients and healthy controls differently. For the healthy controls both CCI and CSI are slightly reduced after the PVT, whereas the CCI and CSI results for the mTBI patients show the opposite trend.

The self-reported fatigue is significantly correlated with CCI in thalamus and CSI in medial frontal gyri. The brain regions showing significant correlations between resting-state functional connectivity and VAS-f overlap largely with the brain areas found to show significant group difference between mTBI patients and healthy controls as identified by 3-way ANOVA.

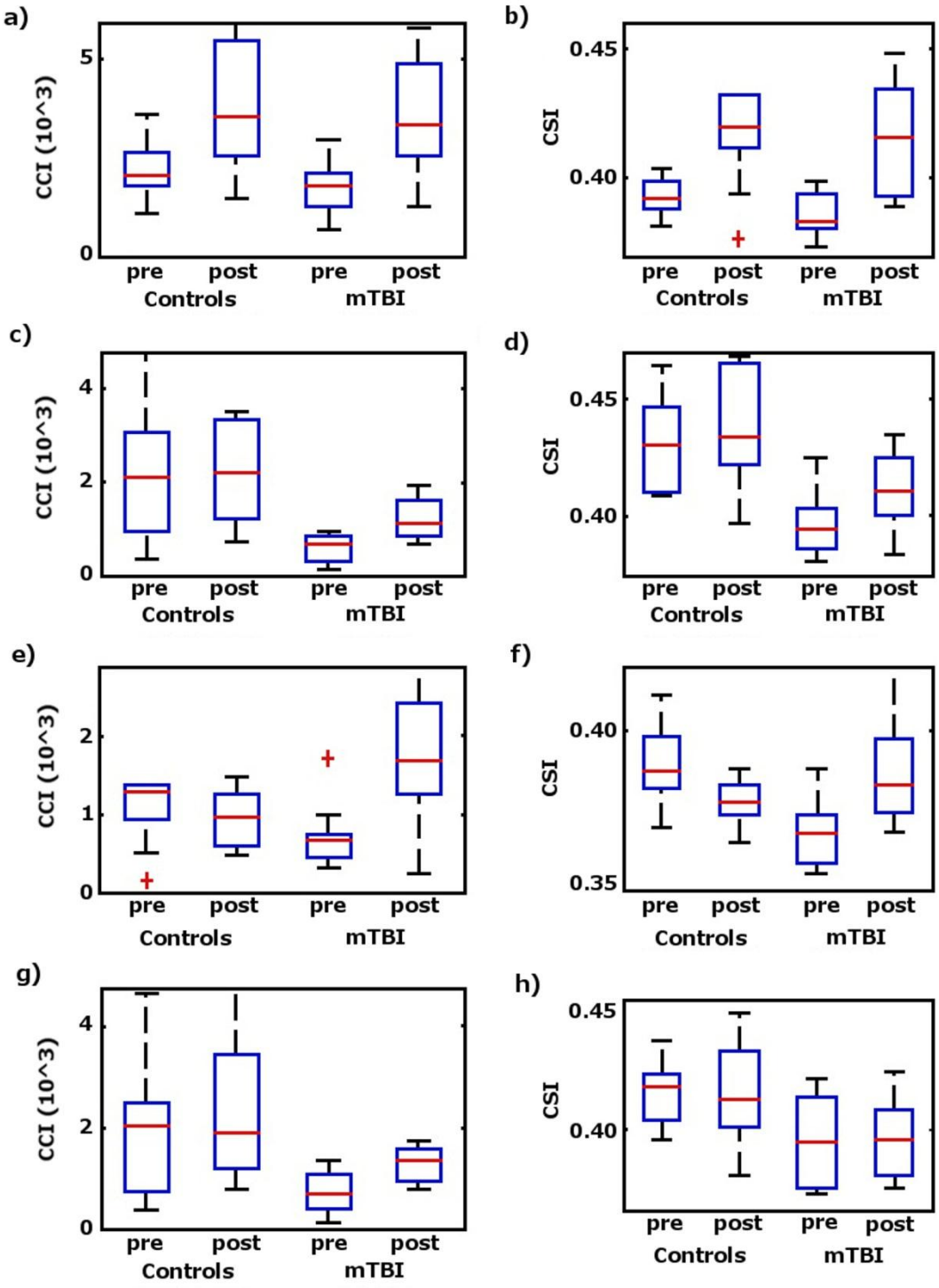

Figure 8 Boxplots of the ROI averages of CCI and CSI for the brain regions with significant effects of PVT and subject group and their interactions. (a) The effect of the PVT on CCI; (b) The effect of the PVT on CSI; (c) CCI difference between mTBI patients and healthy controls; (d) CSI difference between mTBI patients and healthy controls; (e) The interaction effect of CCI showing that mTBI patients and healthy controls are affected differently by the PVT performance; (f) The interaction effect of CSI showing that mTBI patients and healthy controls are affected differently by the PVT; (g) Average CCI for ROIs with significant correlation with VAS-f; (h) Average CSI for ROIs with significant correlation with VAS-f. The central marks of the boxplots show the median, the edges of the box show the 25th and 75th percentiles, the whiskers extend to the most extreme data points that are not considered as outliers, and the outliers are plotted individually as red crosses.

Table 4 List of brain regions with significant statistical contrast as identified by voxel-wise 3-way ANOVA of CCI data and linear regression analysis of CCI and CSI against self-reported current fatigue. X- Y- and Z represent the peak locations of ROIs in the standard MNI coordinates.

	Statistical contrast	ROI	Volume (voxel)	X (mm)	Y (mm)	Z (mm)	Location label
CCI	**Group**	1	30	-11.5	+7.5	+6.5	L-/R-thalamus
	PVT	2	1368	-2.5	+75.0	+2.0	L-/R-cuneus
		3	844	+24.5	+39.5	+62.5	L-pre/postcentral gyrus
		4	528	-51.5	+7.5	+63.0	R-pre/postcentral gyrus
		5	112	-15.5	-4.5	-17.5	R-parahippocampal gyrus
		6	88	-35.5	-4.5	+17.5	R-superior temporal gyrus
		7	69	+0.5	+32.5	-17.5	L-medial frontal gyrus
		8	28	+62.5	-20.5	-5.5	L-inferior frontal gyrus
		9	23	+41.0	+28.0	+7.0	L-middle occipital gyrus
		10	22	+67.0	+20.0	+3.0	L-parahippocampal gyrus
	Interaction	11	20	+4.5	-36.5	+6.5	L-anterior cingulate
		12	13	+52.5	+71.5	-13.5	R-anterior cingulate
CSI	**Group**	1	29	+0.5	-44.5	+30.5	R-medial frontal gyrus
	PVT	2	245	-23.5	+31.5	+54.5	R-postcentral gyrus
		3	163	-19.5	+87.5	-17.5	R-fusiform gyrus
		4	53	-43.5	+23.5	+10.5	R-superior temporal gyrus
		5	35	-15.5	+47.5	+66.5	R-lingual gyrus
		6	32	+26.0	+33.5	+56.0	L-postcentral gyrus
		7	30	-47.5	+63.5	-1.5	R-middle temporal gyrus
		8	29	+5.5	-3.0	+49.0	L-/R-cingulate gyrus
		9	21	+44.5	+27.5	+6.5	L-superior temporal gyrus
	Interaction	10	20	-7.5	-32.5	-1.5	L-/R-anterior cingulate

4.6 DISCUSSION STUDY III

In study III it has been shown that post mTBI fatigue in the chronic phase is significantly correlated with abnormal brain functional connectivity in the thalamus and medial frontal gyri. It was also concluded that a 20 min PVT is sufficient to invoke statistically significant differences in mental fatigue and specific functional connectivity changes in mTBI patients. The deviation of functional connections in the thalamus and medial frontal gyri among mTBI patients is supported by several studies where it has been shown that thalamus plays an important role in the brain's functional connectivity and acts a central hub for information flow control between different subcortical areas and the cerebral cortex (Mastropasqua, Bozzali, Spano, Koch, & Cercignani, 2015; Park & Friston, 2013; Yuan et al., 2015). The thalamus plays an important part in motor control, processing of different sensory signals and maintaining homeostasis of autonomic processes.

Medial frontal gyri have been identified as the site of convergence of dorsal and ventral attention networks and it plays a central role in endogenous and exogenous attention controls (Leung, Gore, & Goldman-Rakic, 2002; Yuan et al., 2015). Reduced CSI of medial frontal

gyri in mTBI patients implicates a lowered intrinsic functional synchronization within the attention networks. Similar results have been shown in previous neuropsychological studies where fatigue was related to reduced processing speed (Gronwall, 1989), higher order attention (Ziino & Ponsford, 2006) and executive functions (van der Linden, Frese, & Meijman, 2003). It is reasonable that mild brain structural injuries in mTBI can lead to disruption of functional networks involving thalamus, medial frontal gyri and lowered efficiency in the performance of complex cognitive tasks. Increase of brain functional connectivity to the thalamus has previously been reported for mTBI patients in the sub-acute phase (Tang et al., 2011).

The PVT resulted in significant performance variability in mTBI patients and significant self-reported "current" fatigue after the task. The PVT induced functional connectivity increases in a number of brain functional networks including sensorimotor cortices, visual cortex, basal ganglia, and fronto-parietal attention network. The up-regulating of resting-state functional connectivity directly after PVT was achieved largely by recruitment of additional components as evidenced by the larger volume increase in CCI compared to CSI.

With the QDA approach, we can perform direct correlation analysis between fatigue assessments and functional connectivity indices to identify the brain regions where fatigue complaints are associated with the change in functional connectivity. The brain regions with significant functional connectivity differences between the two subject groups overlaps largely with the regions with significant linear correlations between fatigue and functional connectivity. This implies that the brain regions with disrupted functional connectivity and group differences play a direct role in executing the task load giving rise to mental fatigue and cognitive fatigability. The correlation results do not necessarily imply causality, but the negative correlation coefficients between fatigue and functional connectivity indices in thalamus and medial frontal gyri indicate that fatigue is accompanied with local resource depletion within the involved functional networks (Brzezicka, Kaminski, & Wrobel, 2013). The correlation results reported in study III are quite consistent with the findings from a previous ASL fMRI study on healthy volunteers where a similar PVT was used (Lim et al., 2010). It was reported that the PVT activated the thalamus and a fronto-parietal attention network involving right middle frontal gyrus in addition to the basal ganglia and sensorimotor cortices. The regional CBF in the medial frontal gyrus attention network was negatively correlated with performance decline.

The change of functional connectivity in the dorsal anterior cingulate cortex before and after the PVT task has a significant interaction effect between group and the PVT task. Both CCI and CSI were down regulated for the healthy controls after the PVT, whereas the opposite trend was observed for the mTBI patient group. Dorsal anterior cingulate cortex is generally active in task settings that are experienced as cognitively difficult and is importantly involved in signaling the occurrence of conflicts in information processing (M. M. Botvinick, Cohen, & Carter, 2004). The function of dorsal anterior cingulate cortex has been hypothesized to monitor conflict as an index of difficulty, evaluate effort demand and outcome, and thereby

trigger compensatory adjustments in cognitive control (M. Botvinick, Nystrom, Fissell, Carter, & Cohen, 1999; M. M. Botvinick et al., 2004; Carter et al., 1998). The down-regulating trend in the healthy controls is likely due to the skill learning effect leading to signaling of reduced effort, while the up-regulating change in the mTBI patients is probably because of the reduced efficiency resulting in signaling of increased effort demand and regulation of effort (Dobryakova, DeLuca, Genova, & Wylie, 2013).

In this current study we have made direct comparison of functional connectivity of mTBI patients and healthy controls measured before and after a PVT. A larger sample size would likely produce more robust results from the linear regression analysis. To compensate for this we recruited a control group matched for age, gender and years of education. We attempted to exclude confounding factors, such as the presence of psychiatric conditions, history of earlier brain pathology, and substance abuse. Overall, the results show promise for further investigations regarding the behavioral correlates of changes in brain functional connectivity.

4.7 RESULTS STUDY IV

In study IV we have investigated CBF differences between post mTBI fatigue patients and healthy controls while performing a demanding sustained attention task in the MRI scanner.

The results from the fatigue measures are the same as reported in study III. In this study the effect of PVT task has been further analyzed by dividing the rCBF results during the performance of PVT into five 4 minute-long quintiles. The mean reaction time and rCBF for each interval were evaluated. The mean reaction time per quintile increased for the patients but remained stable for the controls. It has also been shown that the shorter mean reaction time and less scattering in the reaction times are significantly correlated with the increased self-rated fatigue in patients. General self-rated fatigue and sleep disturbances were not related to performance measures on the PVT for patients or controls.

The results from the 3-way ANOVA (figure 9) show significant changes in rCBF with the increased time on performing PVT in several brain regions including the right thalamus, left supramarginal gyrus and left precuneus. Significant interaction effects between the time of task performance and subject groups were also found in several brain regions including the left thalamus, bilateral medial frontal gyri and right insula.

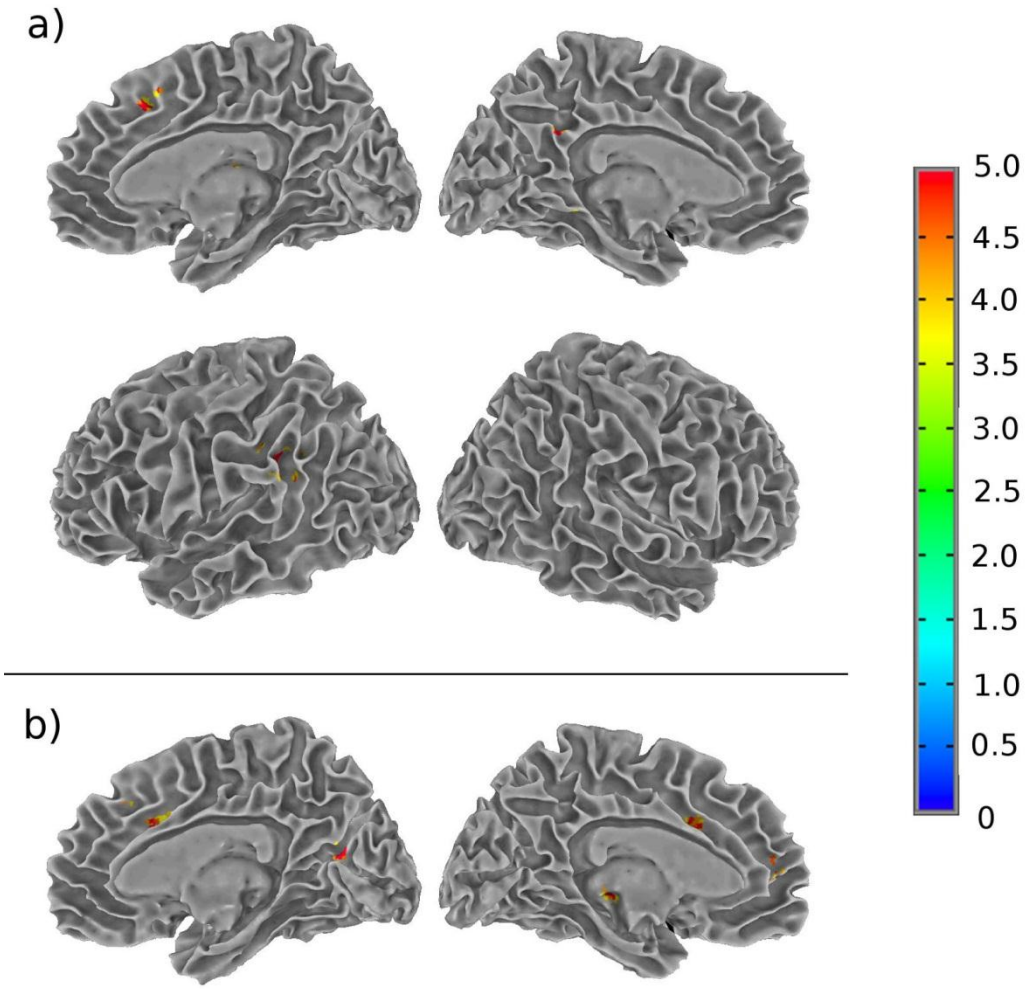

Figure 9 Significant regions from the 3-way ANOVA show (a) the time effect and (b) the interaction effect between time and group.

No significant group effects emerged at a p-value of 0.01. When the p-value threshold was lowered to 0.05 group effects were observed in several brain regions, such as the left middle frontal gyrus, right medial frontal gyrus and right inferior frontal gyrus.

The voxel-wise linear regression analysis showed that there was a significant correlation between rCBF and reaction time during quintile 5 for patients in the right medial frontal gyrus. Significant correlation was also detected between rCBF and the standard deviation of the reaction time during quintile 2 for patients in the left middle frontal gyrus.

Significant correlations between rCBF and post PVT VAS-f rating were also observed in several brain regions for the mTBI patients (figure 10) but no similar correlation emerged for the controls or the entire subject group.

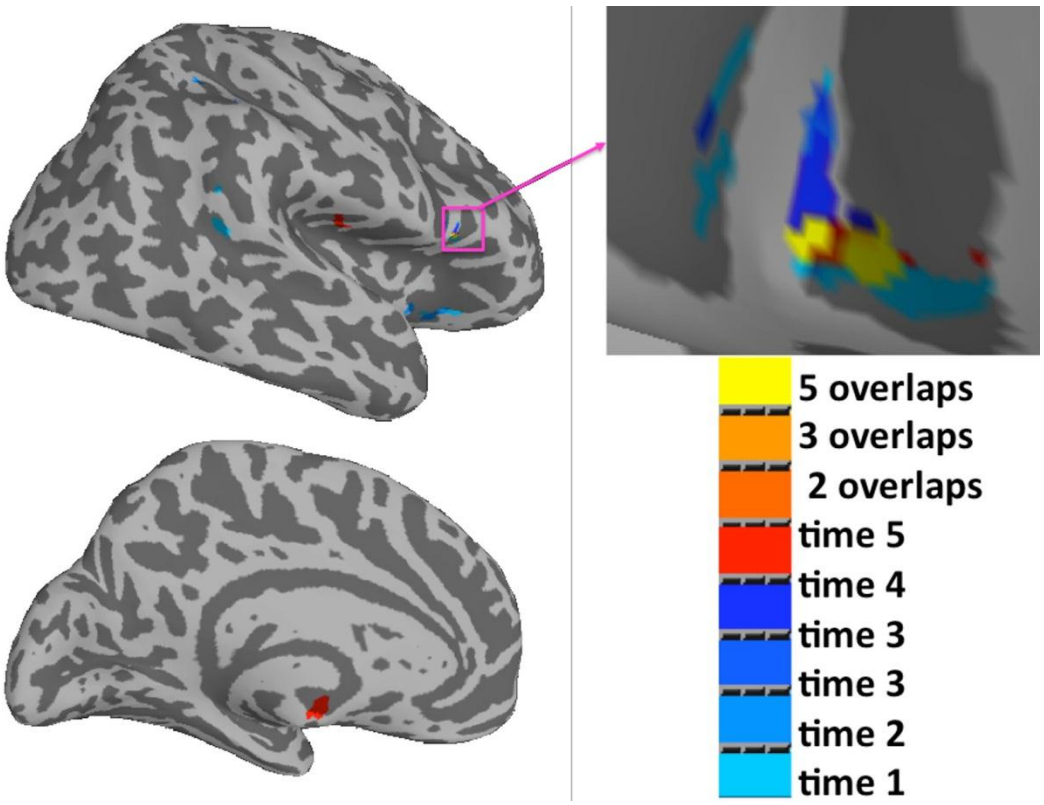

Figure 10 Brain regions with a significant correlation between CBF and the VAS-f ratings after MRI for mTBI patients. Overlapping regions between different quintiles (time points) are shown in the orange-yellow spectrum.

4.8 DISCUSSION STUDY IV

In study IV we had several interesting findings related to fatigue among mTBI patients. The patients showed significantly increased fatigability on the reaction time test as a function of time on performing the task. This was not the case for the healthy controls that were stable in their performance. Performance was also more scattered among the patients compared to the healthy controls showing problems regarding the ability to keep a stable performance level among the patients. The patients scored themselves significantly more fatigued after the PVT, before PVT there was no difference between patients and controls. A correlation was shown between the self-perceived fatigue and fatigability on the PVT for the controls but not for the patients. This suggests that the patients were less able to evaluate fatigability in relation to the change in performance level, indicating probable decreased self-awareness/insight. This was furthermore demonstrated by the fact that the patients that scored a higher increase in fatigue performed better on the PVT task in relation to the patient group as a whole.

The results from the ANOVA analysis on CBF changes during the PVT in study IV show that brain regions including left thalamus, left/right medial frontal gyri and right insula have a significant interaction effect between subject group and time. This indicates that the patients had different processing patterns compared to the controls. These brain regions are also significantly correlated with self-reported fatigue and cognitive fatigability in studies on other patient groups (Dobryakova et al., 2013). The interaction effects in thalamus and medial frontal gyri from this present study are also similar to the results reported in study III (Nordin

et al., 2016). This indicates that changes in functional connectivity as measured by BOLD fMRI are also reflected in CBF changes. Significant changes in CBF over time were found in several brain regions including right thalamus, left supramarginal gyrus and left precuneus for both groups, indicating an increase in functional activity in those areas during a sustained attention task.

When the p-value threshold was decreased to 0.05, group effects were observed in several brain regions such as left middle frontal gyrus, right medial frontal gyrus and right inferior frontal gyrus. Thus, additional group differences, although with lower probability, were found in adjacent frontal areas. The inability to maintain a stable reaction time of PVT over time among patients and altered blood flow in the medial frontal gyrus is interesting because it coincides with the areas of the brain believed to be related to energizing (Stuss, 2011). This region was also strongly related to subjective fatigue after the PVT among patients, but not the controls.

The self-rated current fatigue (VAS-f) after PVT correlated significantly to CBF in several brain regions including right inferior frontal gyrus, right lentiform nucleus, insula and left inferior parietal lobule for the patient group. In a previous study on mental fatigue alterations of the spontaneous oscillatory magnetoencephalography activities was found in right inferior frontal gyrus and left inferior parietal lobule following fatigue-inducing mental tasks (Shigihara et al., 2013). Since we were able to find correlations between CBF and experienced fatigue in the same regions, this implies that the right inferior frontal gyrus and left inferior parietal lobule are involved in the neural mechanisms underlying mental fatigue induced by the PVT. The relationship between cognitive fatigability and performance level is complex. The individual is capable to compensate for fatigue to some extent by applying more effort to maintain his/hers habitual cognitive performance, as indicated by higher autonomic arousal such as elevated diastolic blood pressure (Ziino & Ponsford, 2006). In study IV it was demonstrated that the patients that performed best on the PVT scored higher fatigue after the PVT, which could be interpreted as the slowest patients had a lower overall level of functioning including self-awareness.

A limitation with this study is the relatively small number of participants, as discussed in study III, we compensated for this by recruiting a matched control group considering age, gender and years of education. We normalized the CBF data from the PVT to the resting-state CBF in order to minimize inter-subject differences in base-line CBF. By performing normalization the statistical significance can thus be improved (Aslan & Lu, 2010). We have been able to find several interesting results from this study, both at group level and as a function of time for all subjects, however larger sample sizes would further increase the possibility to detect group differences between mTBI patients and healthy controls using ASL.

5 GENERAL DISCUSSION

The results from these studies show that the pCASL technique is a relatively robust method for quantitative measurements of rCBF in both normal volunteers and patient subjects. Repeated rCBF measurements with the pCASL method is a non-invasive and sufficiently sensitive approach to assess pharmacokinetic response to CNS active chemicals and should be useful for studying the neurophysiological characteristics *in vivo* of potential CNS drugs. The results from the mTBI subjects demonstrate that the repeated measurements of rCBF and functional connectivity metrics before and after a PVT provide sensitive diagnostic imaging methods to assess neurological abnormality of mTBI patients without apparent neuroanatomical damage.

As for all research methods, fMRI techniques have limitations. Some of them are of technical origin and some of physiological origin. By knowing and understanding the limitations with a technique it is possible to improve the methods to minimize the effect of the limitations. This can be done both by technical development of the acquisition methods, adapting the post processing of the acquired data and by implementing appropriate routines to the experimental design.

The results from study I suggests that SNR limits the spatial resolution of rCBF measurements by pCASL pulse sequences. In order to improve the SNR of perfusion measurements several measures can be taken. Both the blood T1 relaxation time and the net magnetization will be increased by using a 3T scanner compared to a 1.5T scanner (J. Wang et al., 2002). SNR can be further improved by using a multi-channel phased-array head coil and by choosing an up to date pulse sequence. Appropriate analysis methods should also be used, for example ROI based analysis, or by enforcing a suitable cluster size for voxel-based analysis to increase SNR. The major reason why the ASL technique suffers from poor SNR is because of the small volume fraction of cerebral blood flow and the inherent subtraction between labeled- and control scans. However, the pair-wise subtraction also has its advantages in reducing the low frequency noise and baseline drift (Detre, Rao, Wang, Chen, & Wang, 2012; Detre & Wang, 2002; Z. Wang, Aguirre, et al., 2008).

It has been shown in several studies that caffeine intake result in a decrease in global rCBF by 20-34.5%, changes in functional connectivity as measured by BOLD fMRI and a decrease of the BOLD signal by 22-37% (Haller et al., 2013; D. J. Wang, Chen, Fernández-Seara, & Detre, 2011). However, abstinence from caffeine can also cause a decrease in global CBF by 33-34.2% (Addicott & Laurienti, 2009; Addicott, Peiffer, & Laurienti, 2012). Increases in rCBF caused by abstinence from nicotine have been shown in brain regions that are important in attention, behavioral control, memory and reward, (Z. Wang et al., 2007; Z. Wang, Ray, et al., 2008). It is not trivial to decide whether to prevent the use of caffeine and/or nicotine or not among subjects participating in fMRI studies. In the studies presented in this thesis we chose to allow the subjects to have one coffee or tea in connection with the fMRI study if they were used to caffeine intake. No nicotine intake was allowed during the study. All nicotine- and caffeine consumption during the study period was recorded. The reasons for

these decisions were; 1) to avoid abstinence effects; 2) we could imagine compliance difficulties from the chronically fatigued patients if they were totally restricted from caffeine. By using relative- instead of absolute CBF data it is possible to avoid effects from caffeine consumption and non-neural factors such as breathing pattern and physiologic state (Aslan & Lu, 2010). This can be done by e.g. normalizing the rCBF data to the whole brain mean CBF or by voxel-wise normalization to perfusion data acquired during resting-state conditions. By performing normalization the noise can be reduced in group comparisons and the statistical significance can be improved.

As discussed in study I, the cerebral blood flow depends on both gender and age. A global decrease of GM and WM CBF with age has been shown along with an increase of the arterial transit time with age and a shorter arterial transit time for women compared to men independent of age (Liu et al., 2012). A decrease in GM-WM CBF ratio with age, mainly depending on the decrease of GM CBF, has been shown by Parkes et al 2004 where higher whole brain CBF among females was also reported (Parkes et al., 2004). A lower CBF in GM and WM has been shown in a group of adults compared to a group of children (Biagi et al., 2007). A strong dependence of T1 and M_0 in cortical GM and changes of the hemodynamic properties of CBF has been shown by Hales et al 2014, where it was claimed that the ASL sequence have to be adopted to children in order to not overestimate CBF among children (Hales, Kawadler, Aylett, Kirkham, & Clark, 2014). The reported differences in whole brain CBF that are related to gender varies between 10-40%. The reason for this difference is still unclear but a lower hematocrit among women causing a reduced oxygen carrying capacity and blood viscosity has been hypothesized (Liu et al., 2012) as well as hormonal influences (Kastrup, Li, Glover, Krüger, & Moseley, 1999). The reported decrease in GM CBF with age varies from 4.5-7.7% per decade in different studies. The reasons for age related changes have been hypothesized to result from neuronal loss (De Vis et al., 2015), a decrease in arterial arrival time, capillary permeability and T_1 of blood (Parkes et al., 2004).

Dependence of age and gender has also been shown for the BOLD signal. A general decrease of the regional homogeneity of synchronicity in the resting-state brain activity with age and a greater local connectivity for females has been shown (Lopez-Larson, Anderson, Ferguson, & Yurgelun-Todd, 2011). The age-related decrease in homogeneity in the resting-state brain activity might be a result of the brain maturation process where the brain efficiency is improved and redundancy is removed (Lopez-Larson et al., 2011). In a study by De Vis et al. 2015 a decrease in cerebrovascular reactivity with age, measured by BOLD fMRI, was shown along with a decrease in whole brain CBF with age, measured by pCASL (De Vis et al., 2015). A higher BOLD contrast and higher regional CBF has been reported for female subjects compared to male subjects following a visual fMRI stimuli (Kastrup, Li, Glover, Krüger, et al., 1999).

In Study I included in this thesis, all subjects were adults and the age span was moderate (average age 34±8 years). A large part of the CBF variation however likely comes from the variety in age and gender among the test subjects. Further studies are needed to investigate

the reasons for CBF variation with age and gender. Individualized ASL sequences may eliminate some of these differences. In study II we recruited only young, adult male subjects in order to avoid gender differences and minimize age variances. There are disadvantages in performing pharmaceutical studies solely on young adult male subjects. Pharmaceutical models need to be accurate for the entire population that the pharmaceuticals under development are intended for. Therefore study II should be considered as a first step towards using pCASL to create a reliable pharmacokinetic/pharmacodynamic model. Further research is needed to generate models that are applicable on a wider population. In study III and IV we recruited a control group matched for both age and gender to minimize the variability in CBF and connectivity that comes from age- and gender dependent factors. The results from study III may still be affected by hormonal differences in the female participants due to the menstrual cycle. In study IV the CBF data was normalized to each individual's CBF during resting-state which should further minimize these effects.

It will never be possible to eliminate all technical limitations with fMRI techniques, or to avoid all physiological variations in BOLD signal or CBF occurring because of other reasons than what is studied. By knowing about the confounding factors it is possible to take measures to minimize the effects of them, to make correct interpretations of the study results and to avoid reporting false positives.

6 SUMMARY AND FUTURE ASPECTS

We have used two brain functional imaging techniques: ASL and resting-sate BOLD fMRI to study the neurological changes in response to the intake of a CNS active drug in healthy volunteers and the neurological abnormalities in mTBI patients with chronic fatigue. The results from the studies presented in this thesis may, in addition to their clinical value, contribute to important knowledge in the design of future functional MRI studies when it comes to determining the study sample size, choosing an appropriate imaging protocol and MRI post processing methods.

The results from study I show that the inter-subject variability is about 2-3 times of that for intra-subject. The intra-subject variability is mainly of SNR origin while both physiological difference and instrumental errors contribute substantially to the inter-subject variability. If the expected pharmacokinetic effect on rCBF for an individual is larger than 10%, pCASL can be a useful method for longitudinal and quantitative studies in monitoring longitudinal changes associated with disease progression or treatment response in clinical trials.

In study II we have shown that the pCASL technique provides useful data to create reliable pharmacokinetic/pharmacodynamic models to assess the pharmacodynamic regional effects of CNS-active drugs. The results from this study show that rCBF changes of 15-20% can be detected in a group of 12 subjects in a placebo controlled pCASL study.

In study III we used a QDA approach to analyze resting-state BOLD fMRI data acquired in mTBI patients before and after the performance of a PVT, which allowed for direct comparisons of functional connectivity measured before and after PVT. The major findings of the study are: post mTBI fatigue in the chronic phase is significantly correlated with abnormal brain functional connectivity in the thalamus and medial frontal gyri, a 20 min PVT is sufficient to invoke statistically significant differences in mental fatigue, specific functional connectivity changes in mTBI patients and resting-state fMRI combined with QDA is a sensitive method for detecting abnormalities in brain functional connectivity of mTBI patients.

In study IV we have shown that pCASL is a suitable technique to investigate neural correlates during a sustained PVT. The major findings from this study are that mTBI patients suffering from fatigue show progressively slower performance speed during a psychomotor vigilance task, that the relationship between self-reported fatigue and performance differs between mTBI patients and controls and that this was associated to abnormal rCBF response to the performance of an enduring task for patients compared to the healthy controls.

A better understanding of the mechanisms underlying fatigue following mTBI would be of clinical importance in order to design rehabilitation programs or pharmacological treatments. The results from study III and IV provides new pieces of information to this clinical puzzle.

We have shown that the functional MRI techniques; pCASL and BOLD fMRI, can be used to study both drug and disease effects on the human brain based on study designs with relative small sample sizes when adequate data processing methods are used.

With the rapid ongoing technological development in both hardware and software within the field of MRI, the main limitations associated with these techniques, such as low SNR, physiological interference and limited temporal resolution are improved. In MRI pulse sequence development attempts have been made to optimize for simultaneous acquisition of ASL and BOLD signals (Schmithorst et al., 2014). With this type of combined data acquisition technique the limitations associated with one technique can be compensated by the strengths of the other method. With the development of local excitation it is possible to label arterial blood in a specific artery at a time in order to visualize the perfusion territories of individual brain feeding arteries (Bokkers, De Cocker, van Osch, Hartkamp, & Hendrikse, 2016). SNR has been substantially improved by hardware development such as ultra-high field MRI of 7T or above, digital electronics and the use of phased-array receivers. 64-channel head coils are now available for 3T clinical MRI systems. SNR can also be improved by the development of 3D pulse sequences in combination with new signal sampling strategies (Nielsen & Hernandez-Garcia, 2013). The labeling efficiency for ASL and CBF calculation can be improved by using appropriate scout sequences to determine the arterial blood velocity, arterial transit time, correction of B_0 off-resonance, choosing an appropriate post labeling delay, an optimal angle of the labeling plane, measuring the equilibrium brain tissue magnetization and T1 of blood (Alsop et al., 2015; Luh et al., 2013; J. Wang et al., 2003; Warmuth, Gunther, & Zimmer, 2003). In order to individualize the ASL sequences with respect to all these factors, fast and accurate imaging protocols are required.

The limitations in temporal resolution for BOLD fMRI can be drastically improved by using ultra-fast MR encephalography which makes it possible to acquire whole brain BOLD activity in 100 ms, i.e. a sampling rate of 10 Hz (Zahneisen et al., 2011). This has been shown, among others, by Rajna et al in 2015 who studied avalanche type activity spreads in the default mode network during resting-state using an under-sampled 3D spiral single-shot sequence (Rajna, Kananen, Keskinarkaus, Seppänen, & Kiviniemi, 2015).

Historically, technical breakthrough has played an important role in the progress of science. The advent of MRI technology in general and functional MRI in particular has made non-invasive studies on human brain structure, function and cognition possible. The future MRI technological progresses in combination with the rapid expansion of computational power will certainly allow for more rapid and higher resolution functional MRI scans. Computation-demanding analysis methods, such as QDA, will also be applicable for large population studies, which can lead to better understanding of cognitive function in relation to drugs, diseases, aging and genetics to mention a few examples.

7 ACKNOWLEDGEMENTS

Thanks to everyone who has contributed to this thesis in any way. In particular I would like to thank the following persons:

My supervisor, ***Tie-Qiang Li***, who has guided me through this work with his incredible expertise within MRI in general and fMRI, ASL, post processing and analysis in particular. I also want to thank my co-supervisor, ***Per Julin***, who has initiated most studies presented in this thesis. Per has been a great source of scientific inspiration.

I especially want to thank my mentor and friend ***Liss-Eric Westman***. Eric has provided great support and he has also made sure I kept physically fit at the gym during my PhD time. I look forward to getting involved in more scientific cooperation with Eric after my dissertation.

Thank you ***Marika Möller*** and ***Aniko Bartfai*** for the collaboration with half of the papers presented in this thesis and the mTBI study. The neuro-psychological perspective that you have provided has certainly enriched this thesis. I look forward to more collaboration in the future.

I want to thank all my ***colleagues*** at the ***Department of MR-Physics***, Karolinska, especially ***Tomas Jonsson*** and former colleague/current friend ***Martin Uppman***. It has been a great pleasure working with you for many years and you have given me plenty of inspiration.

My former boss, ***Leif Svensson***, hired me as an MRI physicist in 2009 and encouraged me to register as a PhD student, thank you for this opportunity.

Peter Aspelin has, in addition to all the help with bureaucratic issues at the institution, functioned as a great source of scientific inspiration and acted as a role model as a scientist.

I want to thank all the ***radiographers*** at the ***MR-department***, Karolinska Huddinge, for the support and giving conversations. I especially want to thank ***Marie Edsborg***, without you it wouldn't have been practically possible or half as enjoyable to accomplish the MRI studies.

Thanks to all my ***colleague*****s** at the ***Department of Medical Physics***, Karolinska Huddinge, you really make me enjoy working at Karolinska.

It would not have been possible to finish this thesis without the extensive help of my ***parents*** and ***in-laws*** who have provided assistance as babysitters in every situation needed.

Most of all, I want to send my special thanks to my beloved family. My wife, ***Linnea Engström Nordin***, never doubted that I would finish this work (which I did myself at times), she has always provided the best support and encouraged me to work with this thesis at hours I should have spent with my family. My daughter, ***Ebba Nordin***, has put my whole world in a new perspective and, even though costing a few hours of sleep, she has given me all the energy I need to finalize this work and move on towards new challenges in life.

Thanks to everyone who has read more of this thesis than just the acknowledgments page ☺

8 REFERENCES

Addicott, M. A., & Laurienti, P. J. (2009). A comparison of the effects of caffeine following abstinence and normal caffeine use. *Psychopharmacology (Berl), 207*(3), 423-431. doi:10.1007/s00213-009-1668-3

Addicott, M. A., Peiffer, A. M., & Laurienti, P. J. (2012). The Effects of Dietary Caffeine Use and Abstention on Blood Oxygen Level-Dependent Activation and Cerebral Blood Flow. *J Caffeine Res, 2*(1), 15-22. doi:10.1089/jcr.2011.0027

Aguirre, G. K., Detre, J. A., Zarahn, E., & Alsop, D. C. (2002). Experimental design and the relative sensitivity of BOLD and perfusion fMRI. *Neuroimage, 15*(3), 488-500. doi:10.1006/nimg.2001.0990

Alsop, D. C., & Detre, J. A. (1998). Multisection cerebral blood flow MR imaging with continuous arterial spin labeling. *Radiology, 208*(2), 410-416. doi:10.1148/radiology.208.2.9680569

Alsop, D. C., Detre, J. A., Golay, X., Günther, M., Hendrikse, J., Hernandez-Garcia, L., . . . Zaharchuk, G. (2015). Recommended implementation of arterial spin-labeled perfusion MRI for clinical applications: A consensus of the ISMRM perfusion study group and the European consortium for ASL in dementia. *Magn Reson Med, 73*(1), 102-116. doi:10.1002/mrm.25197

Aslan, S., & Lu, H. (2010). On the sensitivity of ASL MRI in detecting regional differences in cerebral blood flow. *Magn Reson Imaging, 28*(7), 928-935. doi:10.1016/j.mri.2010.03.037

Bandettini, P. A., Jesmanowicz, A., Wong, E. C., & Hyde, J. S. (1993). Processing strategies for time-course data sets in functional MRI of the human brain. *Magn Reson Med, 30*(2), 161-173.

Bangen, K. J., Restom, K., Liu, T. T., Jak, A. J., Wierenga, C. E., Salmon, D. P., & Bondi, M. W. (2009). Differential age effects on cerebral blood flow and BOLD response to encoding: associations with cognition and stroke risk. *Neurobiol Aging, 30*(8), 1276-1287. doi:10.1016/j.neurobiolaging.2007.11.012

Biagi, L., Abbruzzese, A., Bianchi, M. C., Alsop, D. C., Del Guerra, A., & Tosetti, M. (2007). Age dependence of cerebral perfusion assessed by magnetic resonance continuous arterial spin labeling. *J Magn Reson Imaging, 25*(4), 696-702. doi:10.1002/jmri.20839

Biswal, B., Yetkin, F. Z., Haughton, V. M., & Hyde, J. S. (1995). Functional connectivity in the motor cortex of resting human brain using echo-planar MRI. *Magn Reson Med, 34*(4), 537-541.

Bokkers, R. P., De Cocker, L. J., van Osch, M. J., Hartkamp, N. S., & Hendrikse, J. (2016). Selective Arterial Spin Labeling: Techniques and Neurovascular Applications. *Top Magn Reson Imaging, 25*(2), 73-80. doi:10.1097/RMR.0000000000000078

Botvinick, M., Nystrom, L. E., Fissell, K., Carter, C. S., & Cohen, J. D. (1999). Conflict monitoring versus selection-for-action in anterior cingulate cortex. *Nature, 402*(6758), 179-181. doi:10.1038/46035

Botvinick, M. M., Cohen, J. D., & Carter, C. S. (2004). Conflict monitoring and anterior cingulate cortex: an update. *Trends Cogn Sci, 8*(12), 539-546. doi:10.1016/j.tics.2004.10.003

Bruns, A., Kunnecke, B., Risterucci, C., Moreau, J. L., & von Kienlin, M. (2009). Validation of cerebral blood perfusion imaging as a modality for quantitative pharmacological MRI in rats. *Magn Reson Med, 61*(6), 1451-1458. doi:10.1002/mrm.21779

Brzezicka, A., Kaminski, J., & Wrobel, A. (2013). Local resource depletion hypothesis as a mechanism for action selection in the brain. *Behav Brain Sci, 36*(6), 682-683; discussion 707-626. doi:10.1017/S0140525X13000940

Buxton, R. B., Uludağ, K., Dubowitz, D. J., & Liu, T. T. (2004). Modeling the hemodynamic response to brain activation. *Neuroimage, 23 Suppl 1*, S220-233. doi:10.1016/j.neuroimage.2004.07.013

Buxton, R. B., Wong, E. C., & Frank, L. R. (1998). Dynamics of blood flow and oxygenation changes during brain activation: the balloon model. *Magn Reson Med, 39*(6), 855-864.

Calhoun, V. D., Adali, T., Pearlson, G. D., & Pekar, J. J. (2001). A method for making group inferences from functional MRI data using independent component analysis. *Hum Brain Mapp, 14*(3), 140-151.

Carroll, T. J., Teneggi, V., Jobin, M., Squassante, L., Treyer, V., Hany, T. F., . . . Buck, A. (2002). Absolute quantification of cerebral blood flow with magnetic resonance, reproducibility of the method, and comparison with H2(15)O positron emission tomography. *Journal of cerebral blood flow and metabolism : official journal of the International Society of Cerebral Blood Flow and Metabolism, 22*(9), 1149-1156. doi:10.1097/00004647-200209000-00013

Carter, C. S., Braver, T. S., Barch, D. M., Botvinick, M. M., Noll, D., & Cohen, J. D. (1998). Anterior cingulate cortex, error detection, and the online monitoring of performance. *Science, 280*(5364), 747-749.

Cassidy, J. D., Carroll, L. J., Peloso, P. M., Borg, J., von Holst, H., Holm, L., . . . Injury, W. H. O. C. C. T. F. o. M. T. B. (2004). Incidence, risk factors and prevention of mild traumatic brain injury: results of the WHO Collaborating Centre Task Force on Mild Traumatic Brain Injury. *J Rehabil Med*(43 Suppl), 28-60.

Chaudhuri, A., & Behan, P. O. (2004). Fatigue in neurological disorders. *Lancet, 363*(9413), 978-988. doi:10.1016/S0140-6736(04)15794-2

Chen, J. E., & Glover, G. H. (2015). Functional Magnetic Resonance Imaging Methods. *Neuropsychol Rev, 25*(3), 289-313. doi:10.1007/s11065-015-9294-9

Chen, Y., Wan, H. I., O'Reardon, J. P., Wang, D. J., Wang, Z., Korczykowski, M., & Detre, J. A. (2011). Quantification of cerebral blood flow as biomarker of drug effect: arterial spin labeling phMRI after a single dose of oral citalopram. *Clin Pharmacol Ther, 89*(2), 251-258. doi:10.1038/clpt.2010.296

Cordes, D., Haughton, V. M., Arfanakis, K., Wendt, G. J., Turski, P. A., Moritz, C. H., . . . Meyerand, M. E. (2000). Mapping functionally related regions of brain with functional connectivity MR imaging. *AJNR Am J Neuroradiol, 21*(9), 1636-1644.

Dai, W., Garcia, D., de Bazelaire, C., & Alsop, D. C. (2008). Continuous flow-driven inversion for arterial spin labeling using pulsed radio frequency and gradient fields. *Magn Reson Med, 60*(6), 1488-1497. doi:10.1002/mrm.21790

De Vis, J. B., Hendrikse, J., Bhogal, A., Adams, A., Kappelle, L. J., & Petersen, E. T. (2015). Age-related changes in brain hemodynamics; A calibrated MRI study. *Hum Brain Mapp, 36*(10), 3973-3987. doi:10.1002/hbm.22891

Detre, J. A., Leigh, J. S., Williams, D. S., & Koretsky, A. P. (1992). Perfusion imaging. *Magn Reson Med, 23*(1), 37-45.

Detre, J. A., Rao, H., Wang, D. J., Chen, Y. F., & Wang, Z. (2012). Applications of arterial spin labeled MRI in the brain. *J Magn Reson Imaging, 35*(5), 1026-1037. doi:10.1002/jmri.23581

Detre, J. A., & Wang, J. (2002). Technical aspects and utility of fMRI using BOLD and ASL. *Clin Neurophysiol, 113*(5), 621-634.

Detre, J. A., Zhang, W., Roberts, D. A., Silva, A. C., Williams, D. S., Grandis, D. J., . . . Leigh, J. S. (1994). Tissue specific perfusion imaging using arterial spin labeling. *NMR Biomed, 7*(1-2), 75-82.

Devous, M. D., Sr., Trivedi, M. H., & Rush, A. J. (2001). Regional cerebral blood flow response to oral amphetamine challenge in healthy volunteers. *J Nucl Med, 42*(4), 535-542.

Dobryakova, E., DeLuca, J., Genova, H. M., & Wylie, G. R. (2013). Neural correlates of cognitive fatigue: cortico-striatal circuitry and effort-reward imbalance. *J Int Neuropsychol Soc, 19*(8), 849-853. doi:10.1017/S1355617713000684

Eklund, A., Nichols, T. E., & Knutsson, H. (2016). Cluster failure: Why fMRI inferences for spatial extent have inflated false-positive rates. *Proc Natl Acad Sci U S A*. doi:10.1073/pnas.1602413113

Frank, L. R., Wong, E. C., & Buxton, R. B. (1997). Slice profile effects in adiabatic inversion: application to multislice perfusion imaging. *Magn Reson Med, 38*(4), 558-564.

Friston, K. J., Holmes, A. P., Poline, J. B., Grasby, P. J., Williams, S. C., Frackowiak, R. S., & Turner, R. (1995). Analysis of fMRI time-series revisited. *Neuroimage, 2*(1), 45-53. doi:10.1006/nimg.1995.1007

Golay, X., Hendrikse, J., & Lim, T. C. (2004). Perfusion imaging using arterial spin labeling. *Top Magn Reson Imaging, 15*(1), 10-27.

Grichisch, Y., Cavusoglu, M., Preissl, H., Uludag, K., Hallschmid, M., Birbaumer, N., . . . Veit, R. (2012). Differential effects of intranasal insulin and caffeine on cerebral blood flow. *Hum Brain Mapp, 33*(2), 280-287. doi:10.1002/hbm.21216

Gronwall, D. (1989). Cumulative and persisting effects of concussion on attention and cognition. In H. S. Levin, Eisenberg, H.M., & Benton, A.L. (Ed.), *Mild Head Injury* (pp. 153-162). New York: Oxford University Press.

Hales, P. W., Kawadler, J. M., Aylett, S. E., Kirkham, F. J., & Clark, C. A. (2014). Arterial spin labeling characterization of cerebral perfusion during normal maturation from late childhood into adulthood: normal 'reference range' values and their use in clinical studies. *J Cereb Blood Flow Metab, 34*(5), 776-784. doi:10.1038/jcbfm.2014.17

Haller, S., Rodriguez, C., Moser, D., Toma, S., Hofmeister, J., Sinanaj, I., . . . Lovblad, K. O. (2013). Acute caffeine administration impact on working memory-related brain activation and functional connectivity in the elderly: a BOLD and perfusion MRI study. *Neuroscience, 250*, 364-371. doi:10.1016/j.neuroscience.2013.07.021

Henderson, G., Tomlinson, B. E., & Gibson, P. H. (Eds.). (1980). *Cell counts in human cerebral cortex in normal adults throughout life using an image analysing computer* (Vol. 46). Netherlands.

Hogarth, A. J., Mackintosh, A. F., & Mary, D. A. (Eds.). (2007). *Gender-related differences in the sympathetic vasoconstrictor drive of normal subjects* (Vol. 112). England.

Jahanian, H., Noll, D. C., & Hernandez-Garcia, L. (2011). B0 field inhomogeneity considerations in pseudo-continuous arterial spin labeling (pCASL): effects on tagging efficiency and correction strategy. *NMR Biomed, 24*(10), 1202-1209. doi:10.1002/nbm.1675

Jahng, G. H., Song, E., Zhu, X. P., Matson, G. B., Weiner, M. W., & Schuff, N. (2005). Human brain: reliability and reproducibility of pulsed arterial spin-labeling perfusion MR imaging. *Radiology, 234*, 909-916. doi:10.1148/radiol.2343031499

Kahn, D. A., Prohovnik, I., Lucas, L. R., & Sackeim, H. A. (1989). Dissociated effects of amphetamine on arousal and cortical blood flow in humans. *Biol Psychiatry, 25*(6), 755-767. doi:0006-3223(89)90247-3 [pii]

Kastrup, A., Li, T. Q., Glover, G. H., Kruger, G., & Moseley, M. E. (1999). Gender differences in cerebral blood flow and oxygenation response during focal physiologic neural activity. *Journal of cerebral blood flow and metabolism : official journal of the International Society of Cerebral Blood Flow and Metabolism, 19*(10), 1066-1071. doi:10.1097/00004647-199910000-00002

Kastrup, A., Li, T. Q., Glover, G. H., Krüger, G., & Moseley, M. E. (1999). Gender differences in cerebral blood flow and oxygenation response during focal physiologic neural activity. *J Cereb Blood Flow Metab, 19*(10), 1066-1071. doi:10.1097/00004647-199910000-00002

Khalili-Mahani, N., van Osch, M. J., Baerends, E., Soeter, R. P., de Kam, M., Zoethout, R. W., . . . Rombouts, S. A. (2011). Pseudocontinuous arterial spin labeling reveals dissociable effects of morphine and alcohol on regional cerebral blood flow. *J Cereb Blood Flow Metab, 31*(5), 1321-1333. doi:10.1038/jcbfm.2010.234

Lannsjo, M., af Geijerstam, J. L., Johansson, U., Bring, J., & Borg, J. (2009). Prevalence and structure of symptoms at 3 months after mild traumatic brain injury in a national cohort. *Brain Inj, 23*(3), 213-219. doi:10.1080/02699050902748356

Leung, H. C., Gore, J. C., & Goldman-Rakic, P. S. (2002). Sustained mnemonic response in the human middle frontal gyrus during on-line storage of spatial memoranda. *J Cogn Neurosci, 14*(4), 659-671. doi:10.1162/08989290260045882

Li, T. Q., Haefelin, T. N., Chan, B., Kastrup, A., Jonsson, T., Glover, G. H., & Moseley, M. E. (2000). Assessment of hemodynamic response during focal neural activity in human using bolus tracking, arterial spin labeling and BOLD techniques *Neuroimage* (2000/09/16 ed., Vol. 12, pp. 442-451).

Li, T. Q., Hallin, R., & Juto, J. E. (2015). *Kinetic oscillatory stimulation (KOS) in the nasal cavity studied by resting-state fMRI.* Paper presented at the Proc. ISMRM, Toronto.

Li, T. Q., Kastrup, A., Takahashi, A. M., & Moseley, M. E. (1999). Functional MRI of human brain during breath holding by BOLD and FAIR techniques. *Neuroimage, 9*(2), 243-249.

Li, T. Q., Moseley, M. E., & Glover, G. (1999). A FAIR study of motor cortex activation under normo- and hypercapnia induced by breath challenge. *Neuroimage, 10*(5), 562-569.

Li, Z. J., Matsuda, H., Asada, T., Ohnishi, T., Kanetaka, H., Imabayashi, E., & Tanaka, F. (Eds.). (2004). *Gender difference in brain perfusion 99mTc-ECD SPECT in aged healthy volunteers after correction for partial volume effects* (Vol. 25). England.

Lim, J., Wu, W. C., Wang, J., Detre, J. A., Dinges, D. F., & Rao, H. (2010). Imaging brain fatigue from sustained mental workload: an ASL perfusion study of the time-on-task effect. *Neuroimage, 49*(4), 3426-3435. doi:10.1016/j.neuroimage.2009.11.020

Liu, Y., Zhu, X., Feinberg, D., Guenther, M., Gregori, J., Weiner, M. W., & Schuff, N. (2012). Arterial spin labeling MRI study of age and gender effects on brain perfusion hemodynamics. *Magn Reson Med, 68*(3), 912-922. doi:10.1002/mrm.23286

Lopez-Larson, M. P., Anderson, J. S., Ferguson, M. A., & Yurgelun-Todd, D. (2011). Local brain connectivity and associations with gender and age. *Dev Cogn Neurosci, 1*(2), 187-197. doi:10.1016/j.dcn.2010.10.001

Lowe, M. J. (2010). A historical perspective on the evolution of resting-state functional connectivity with MRI. *MAGMA, 23*(5-6), 279-288. doi:10.1007/s10334-010-0230-y

Luh, W. M., Talagala, S. L., Li, T. Q., & Bandettini, P. A. (2013). Pseudo-continuous arterial spin labeling at 7 T for human brain: estimation and correction for off-resonance effects using a Prescan. *Magn Reson Med, 69*(2), 402-410. doi:10.1002/mrm.24266

Mansfield, P. (1977). Multi-planar image formation using NMR spin echoes. *Journal of Physics C: Solid State Physics, 10*(3), L55.

Mastropasqua, C., Bozzali, M., Spano, B., Koch, G., & Cercignani, M. (2015). Functional Anatomy of the Thalamus as a Model of Integrated Structural and Functional Connectivity of the Human Brain In Vivo. *Brain Topogr, 28*(4), 548-558. doi:10.1007/s10548-014-0422-2

Mathew, R. J., & Wilson, W. H. (1985). Dextroamphetamine-induced changes in regional cerebral blood flow. *Psychopharmacology (Berl), 87*(3), 298-302.

McKeown, M. J., & Sejnowski, T. J. (1998). Independent component analysis of fMRI data: examining the assumptions. *Hum Brain Mapp, 6*(5-6), 368-372.

Mild Traumatic Brain Injury Committee of the Head Injury Interdisciplinary Special Interest Group of the American Congress of Rehabilitation Medicine: Definition of mild traumatic brain injury. (1993). *Journal of Head Trauma Rehabilitation, 8*(3), 86-87.

Nezamzadeh, M., Matson, G. B., Young, K., Weiner, M. W., & Schuff, N. (2010). Improved pseudo-continuous arterial spin labeling for mapping brain perfusion. *J Magn Reson Imaging, 31*(6), 1419-1427. doi:10.1002/jmri.22199

Nielsen, J. F., & Hernandez-Garcia, L. (2013). Functional perfusion imaging using pseudocontinuous arterial spin labeling with low-flip-angle segmented 3D spiral readouts. *Magn Reson Med, 69*(2), 382-390. doi:10.1002/mrm.24261

Nordin, L. E., Möller, M. C., Julin, P., Bartfai, A., Hashim, F., & Li, T. Q. (2016). Post mTBI fatigue is associated with abnormal brain functional connectivity. *Sci Rep, 6*, 21183. doi:10.1038/srep21183

Ogawa, S., Lee, T. M., Kay, A. R., & Tank, D. W. (1990). Brain magnetic resonance imaging with contrast dependent on blood oxygenation. *Proc Natl Acad Sci U S A, 87*(24), 9868-9872.

Pakkenberg, B., & Gundersen, H. J. (Eds.). (1997). *Neocortical neuron number in humans: effect of sex and age* (Vol. 384). United States.

Park, H. J., & Friston, K. (2013). Structural and functional brain networks: from connections to cognition. *Science, 342*(6158), 1238411. doi:10.1126/science.1238411

Parkes, L. M., Rashid, W., Chard, D. T., & Tofts, P. S. (2004). Normal cerebral perfusion measurements using arterial spin labeling: reproducibility, stability, and age and gender effects. *Magn Reson Med, 51*(4), 736-743. doi:10.1002/mrm.20023

Paulson, O. B., Strandgaard, S., & Edvinsson, L. (1990). Cerebral autoregulation. *Cerebrovasc Brain Metab Rev, 2*(2), 161-192.

Price, J. C., Drevets, W. C., Ruszkiewicz, J., Greer, P. J., Villemagne, V. L., Xu, L., . . . Mathis, C. A. (2002). Sequential H(2)(15)O PET studies in baboons: before and after amphetamine. *J Nucl Med, 43*(8), 1090-1100.

Raichle, M. E., Grubb, R. L., Gado, M. H., Eichling, J. O., & Ter-Pogossian, M. M. (1976). Correlation between regional cerebral blood flow and oxidative metabolism. In vivo studies in man. *Arch Neurol, 33*(8), 523-526.

Rajna, Z., Kananen, J., Keskinarkaus, A., Seppänen, T., & Kiviniemi, V. (2015). Detection of short-term activity avalanches in human brain default mode network with ultrafast MR encephalography. *Front Hum Neurosci, 9*, 448. doi:10.3389/fnhum.2015.00448

Ren, J., Xu, H., Choi, J. K., Jenkins, B. G., & Chen, Y. I. (2009). Dopaminergic response to graded dopamine concentration elicited by four amphetamine doses. *Synapse, 63*(9), 764-772. doi:10.1002/syn.20659

Restom, K., Bangen, K. J., Bondi, M. W., Perthen, J. E., & Liu, T. T. (Eds.). (2007). *Cerebral blood flow and BOLD responses to a memory encoding task: a comparison between healthy young and elderly adults* (Vol. 37). United States.

Rose, S. E., Janke, A. L., Strudwick, M. W., McMahon, K. L., Chalk, J. B., Snyder, P., & De zubicaray, G. I. (2006). Assessment of dynamic susceptibility contrast cerebral blood flow response to amphetamine challenge: A human pharmacological magnetic resonance imaging study at 1.5 and 4 T. *Magnetic Resonance in Medicine, 55*(1), 9-15. doi:10.1002/mrm.20749

Rosenthal, T. C. a. M. B. A. a. P. R. a. M. K. (2008). Fatigue: an overview. *American Family Physician, 78*(10), 1173--1179.

Schmithorst, V. J., Hernandez-Garcia, L., Vannest, J., Rajagopal, A., Lee, G., & Holland, S. K. (2014). Optimized simultaneous ASL and BOLD functional imaging of the whole brain. *J Magn Reson Imaging, 39*(5), 1104-1117. doi:10.1002/jmri.24273

Schouw, M. L., Gevers, S., Caan, M. W., Majoie, C. B., Booij, J., Nederveen, A. J., & Reneman, L. (2011). Mapping serotonergic dysfunction in MDMA (ecstasy) users using pharmacological MRI. *Eur Neuropsychopharmacol*. doi:10.1016/j.euroneuro.2011.12.002

Shigihara, Y., Tanaka, M., Ishii, A., Kanai, E., Funakura, M., & Watanabe, Y. (2013). Two types of mental fatigue affect spontaneous oscillatory brain activities in different ways. *Behav Brain Funct, 9*, 2. doi:10.1186/1744-9081-9-2

Silva, A. C., & Kim, S. G. (1999). Pseudo-continuous arterial spin labeling technique for measuring CBF dynamics with high temporal resolution. *Magn Reson Med, 42*(3), 425-429.

Silva, A. C., Zhang, W., Williams, D. S., & Koretsky, A. P. (1995). Multi-slice MRI of rat brain perfusion during amphetamine stimulation using arterial spin labeling. *Magn Reson Med, 33*(2), 209-214.

Stulemeijer, M., van der Werf, S., Bleijenberg, G., Biert, J., Brauer, J., & Vos, P. E. (2006). Recovery from mild traumatic brain injury: a focus on fatigue. *J Neurol, 253*(8), 1041-1047. doi:10.1007/s00415-006-0156-5

Stuss, D. T. (2011). Functions of the frontal lobes: relation to executive functions. *J Int Neuropsychol Soc, 17*(5), 759-765. doi:10.1017/S1355617711000695

Tang, L., Ge, Y., Sodickson, D. K., Miles, L., Zhou, Y., Reaume, J., & Grossman, R. I. (2011). Thalamic resting-state functional networks: disruption in patients with mild traumatic brain injury. *Radiology, 260*(3), 831-840. doi:10.1148/radiol.11110014

van der Linden, D., Frese, M., & Meijman, T. F. (2003). Mental fatigue and the control of cognitive processes: effects on perseveration and planning. *Acta Psychologica, 113*, 45-65.

Vollenweider, F. X., Maguire, R. P., Leenders, K. L., Mathys, K., & Angst, J. (1998). Effects of high amphetamine dose on mood and cerebral glucose metabolism in normal volunteers using positron emission tomography (PET). *Psychiatry Res, 83*(3), 149-162.

Wang, D. J., Chen, Y., Fernández-Seara, M. A., & Detre, J. A. (2011). Potentials and challenges for arterial spin labeling in pharmacological magnetic resonance imaging. *J Pharmacol Exp Ther, 337*(2), 359-366. doi:10.1124/jpet.110.172577

Wang, J., Aguirre, G. K., Kimberg, D. Y., Roc, A. C., Li, L., & Detre, J. A. (2003). Arterial spin labeling perfusion fMRI with very low task frequency. *Magn Reson Med, 49*(5), 796-802. doi:10.1002/mrm.10437

Wang, J., Alsop, D. C., Li, L., Listerud, J., Gonzalez-At, J. B., Schnall, M. D., & Detre, J. A. (2002). Comparison of quantitative perfusion imaging using arterial spin labeling at 1.5 and 4.0 Tesla. *Magnetic resonance in medicine : official journal of the Society of Magnetic Resonance in Medicine / Society of Magnetic Resonance in Medicine, 48*(2), 242-254. doi:10.1002/mrm.10211

Wang, J., Korczykowski, M., Rao, H., Fan, Y., Pluta, J., Gur, R. C., . . . Detre, J. A. (2007). Gender difference in neural response to psychological stress. *Social cognitive and affective neuroscience, 2*(3), 227-239. doi:10.1093/scan/nsm018

Wang, Y., & Li, T. Q. (2015). Dimensionality of ICA in resting-state fMRI investigated by feature optimized classification of independent components with SVM. *Front Hum Neurosci, 9*, 259. doi:10.3389/fnhum.2015.00259

Wang, Z., Aguirre, G. K., Rao, H., Wang, J., Fernández-Seara, M. A., Childress, A. R., & Detre, J. A. (2008). Empirical optimization of ASL data analysis using an ASL data processing toolbox: ASLtbx. *Magn Reson Imaging, 26*(2), 261-269. doi:10.1016/j.mri.2007.07.003

Wang, Z., Faith, M., Patterson, F., Tang, K., Kerrin, K., Wileyto, E. P., . . . Lerman, C. (2007). Neural substrates of abstinence-induced cigarette cravings in chronic smokers. *J Neurosci, 27*(51), 14035-14040. doi:10.1523/JNEUROSCI.2966-07.2007

Wang, Z., Ray, R., Faith, M., Tang, K., Wileyto, E. P., Detre, J. A., & Lerman, C. (2008). Nicotine abstinence-induced cerebral blood flow changes by genotype. *Neurosci Lett, 438*(3), 275-280. doi:10.1016/j.neulet.2008.04.084

Warmuth, C., Gunther, M., & Zimmer, C. (2003). Quantification of blood flow in brain tumors: comparison of arterial spin labeling and dynamic susceptibility-weighted contrast-enhanced MR imaging. *Radiology, 228*(2), 523-532. doi:10.1148/radiol.2282020409

Williams, D. S., Detre, J. A., Leigh, J. S., & Koretsky, A. P. (1992). Magnetic resonance imaging of perfusion using spin inversion of arterial water. *Proc Natl Acad Sci U S A, 89*(1), 212-216.

Wolkin, A., Angrist, B., Wolf, A., Brodie, J., Wolkin, B., Jaeger, J., . . . Rotrosen, J. (1987). Effects of amphetamine on local cerebral metabolism in normal and schizophrenic subjects as determined by positron emission tomography. *Psychopharmacology (Berl), 92*(2), 241-246.

Wong, E. C., Buxton, R. B., & Frank, L. R. (1997). Implementation of quantitative perfusion imaging techniques for functional brain mapping using pulsed arterial spin labeling. *NMR Biomed, 10*(4-5), 237-249.

Wong, E. C., Buxton, R. B., & Frank, L. R. (1998a). A theoretical and experimental comparison of continuous and pulsed arterial spin labeling techniques for quantitative perfusion imaging. *Magn Reson Med, 40*(3), 348-355.

Wong, E. C., Buxton, R. B., & Frank, L. R. (1998b). Quantitative imaging of perfusion using a single subtraction (QUIPSS and QUIPSS II). *Magn Reson Med, 39*(5), 702-708.

Wu, W. C., Fernández-Seara, M., Detre, J. A., Wehrli, F. W., & Wang, J. (2007). A theoretical and experimental investigation of the tagging efficiency of pseudocontinuous arterial spin labeling. *Magn Reson Med, 58*(5), 1020-1027. doi:10.1002/mrm.21403

Xu, G., Rowley, H. A., Wu, G., Alsop, D. C., Shankaranarayanan, A., Dowling, M., . . . Johnson, S. C. (2010). Reliability and precision of pseudo-continuous arterial spin labeling perfusion MRI on 3.0 T and comparison with 15O-water PET in elderly subjects at risk for Alzheimer's disease. *NMR in biomedicine, 23*(3), 286-293. doi:10.1002/nbm.1462

Ye, F. Q., Berman, K. F., Ellmore, T., Esposito, G., van Horn, J. D., Yang, Y., . . . McLaughlin, A. C. (2000a). H(2)(15)O PET validation of steady-state arterial spin tagging cerebral blood flow measurements in humans. *Magn Reson Med, 44*(3), 450-456.

Ye, F. Q., Berman, K. F., Ellmore, T., Esposito, G., van Horn, J. D., Yang, Y., . . . McLaughlin, A. C. (Eds.). (2000b). *H(2)(15)O PET validation of steady-state arterial spin tagging cerebral blood flow measurements in humans* (Vol. 44). United States.

Yuan, R., Di, X., Taylor, P. A., Gohel, S., Tsai, Y. H., & Biswal, B. B. (2015). Functional topography of the thalamocortical system in human. *Brain Struct Funct*. doi:10.1007/s00429-015-1018-7

Zahneisen, B., Grotz, T., Lee, K. J., Ohlendorf, S., Reisert, M., Zaitsev, M., & Hennig, J. (2011). Three-dimensional MR-encephalography: fast volumetric brain imaging using rosette trajectories. *Magn Reson Med, 65*(5), 1260-1268. doi:10.1002/mrm.22711

Zhang, W., Silva, A. C., Williams, D. S., & Koretsky, A. P. (1995). NMR measurement of perfusion using arterial spin labeling without saturation of macromolecular spins. *Magn Reson Med, 33*(3), 370-376.

Zhang, W., Williams, D. S., & Koretsky, A. P. (1993). Measurement of rat brain perfusion by NMR using spin labeling of arterial water: in vivo determination of the degree of spin labeling. *Magn Reson Med, 29*(3), 416-421.

Ziino, C., & Ponsford, J. (2006). Selective attention deficits and subjective fatigue following traumatic brain injury. *Neuropsychology, 20*(3), 383-390.